REPORT DOCUMENTATION PAGE

Form Approved OMB NO. 0704-0188

1. REPORT DATE (DD-MM-YYYY)	2. REPORT TYPE	3. DATES COVERED (From - To)
10-04-2023	Final Report	1-Jul-2022 - 31-Mar-2023

4. TITLE AND SUBTITLE
Final Report: Structure-property relationships of novel electronic functional materials using contactless probing

5a. CONTRACT NUMBER
W911NF-22-1-0116

5b. GRANT NUMBER

5c. PROGRAM ELEMENT NUMBER
611102

6. AUTHORS

5d. PROJECT NUMBER

5e. TASK NUMBER

5f. WORK UNIT NUMBER

7. PERFORMING ORGANIZATION NAMES AND ADDRESSES
North Carolina Central University
1801 Fayetteville Street

Durham, NC 27707 -3129

8. PERFORMING ORGANIZATION REPORT NUMBER

9. SPONSORING/MONITORING AGENCY NAME(S) AND ADDRESS (ES)
U.S. Army Research Office
P.O. Box 12211
Research Triangle Park, NC 27709-2211

10. SPONSOR/MONITOR'S ACRONYM(S)
ARO

11. SPONSOR/MONITOR'S REPORT NUMBER(S)
80202-EM-II.6

12. DISTRIBUTION AVAILIBILITY STATEMENT
Approved for public release; distribution is unlimited.

13. SUPPLEMENTARY NOTES
The views, opinions and/or findings contained in this report are those of the author(s) and should not contrued as an official Department of the Army position, policy or decision, unless so designated by other documentation.

14. ABSTRACT

15. SUBJECT TERMS

16. SECURITY CLASSIFICATION OF:			17. LIMITATION OF ABSTRACT	15. NUMBER OF PAGES	19a. NAME OF RESPONSIBLE PERSON
a. REPORT	b. ABSTRACT	c. THIS PAGE			Biswadev Roy
UU	UU	UU	UU		19b. TELEPHONE NUMBER 919-599-2043

RPPR Final Report
as of 11-Apr-2023

Agency Code: 21XD

Proposal Number: 80202EMII **Agreement Number: W911NF-22-1-0116**
INVESTIGATOR(S):

Name: Biswadev Roy
Email: broy@nccu.edu
Phone Number: 9195992043
Principal: Y

Organization: **North Carolina Central University**
Address: 1801 Fayetteville Street, Durham, NC 277073129
Country: USA

DUNS Number: 783691801 EIN: 566000730
Report Date: 30-Jun-2023 Date Received: 10-Apr-2023
Final Report for Period Beginning 01-Jul-2022 and Ending 31-Mar-2023
Title: Structure-property relationships of novel electronic functional materials using contactless probing
Begin Performance Period: 01-Jul-2022 **End Performance Period:** 31-Mar-2023
Report Term: 0-Other

Submitted By: Biswadev Roy Email: broy@nccu.edu
Phone: (919) 599-2043

Distribution Statement: 1-Approved for public release; distribution is unlimited.

STEM Degrees: **STEM Participants:** 1

Major Goals: • To establish structure-property-field effect relationships of three different materials viz. indirect band gap hybrid methyl-ammonium lead iodide (MAL3I) with a perovskite structure having indirect band gap ~1.5 eV, a slightly n-type indirect band gap (~1.1eV) Hafnium di-selenide (a transition metal dichalcogenide), and a purely organic acceptor material [6,6]-phenyl-C 61 -butyric acid methyl ester (PCBM) and its electron beam irradiated variant, with optimal band gap 1.3-1.9 eV by subjecting various samples to different temperatures using a well-calibrated cryostat.

- The goals for the MAL3I investigation involve A) how specimen combined Wannier-Mott and Frenkel excitons behave in terms of the changes in external temperature of the sample (influence of spin-orbit coupling and its effect on mobility measured at millimeter wave probe frequencies) for the temperature range 8K-350K and also by age of the sample. B) What is the signal settling time when voltage response and their steady-state differences are ~2% of the peak voltages and how does the positive- to negative photo response voltages behave for studying the extents of sloe- and fast recombination process, C) Whether the shallow trap developments aid in enhancing lifetime as observed at millimeter wave frequencies and does chemical passivation of MAL3I have any pronounced effect on the shape of the conductance kinetics (charge population relationship with mobility). D) To include the structural information from MAL3I investigations to study photo responses.
- The goals of fast switching material group IV TMD Hafnium di-selenide thin film include A) obtaining structural information from the Raman system and SNOM, B) generating averaged photo-transients using millimeter wave pump-probe spectroscopy (TR-mmWC) and study variation of peak voltages with age and structural changes induced due to external temperature, and use the crystals to create test chips for FET measurements and its relationships with the structural changes and millimeter wave response.
- Goals of 99.5% pure electron acceptor material PCBM (Methanofullerene [6,6] – phenyl C61-butyric-acid methyl ester) include: A) studying photo responses using 266nm laser induced millimeter wave probed charge carrier dynamics also at external temperatures 8K-350K. B) to study the effect of 50 keV/1.6 μA electron beam irradiation on 99.5% pure PCBM film on its band structure (effect of alteration of the lowest unoccupied molecular orbital level by electron beam)

The overall objective of the project was to relate the structure of 3 different types of semiconductor thin films viz. aged, and new MAL3I: a hybrid thin film, a CsPbI2Br (perovskite structure, but completely inorganic constitution), a HfSe2 inorganic thin film and PCBM, a purely organic thin film using noise-free averaged transient datasets obtained from using the in-house time-resolved millimeter wave conductivity apparatus in transmission and reflection mode, and, finally relate to their respective field-effect functionality merits for justifying its use as a reliable Field Effect Transistor (FET) material.

Accomplishments: Our major objective was to produce thin films to study photo-physics of 3 novel materials one,

a hybrid perovskite (2 different types of methylammonium lead halide, MAL3I), one inorganic Hafnium-di-selenide (HfSe2), and a completely organic acceptor material (PCB61M). The plan was to acquire time-resolved millimeter wave differential absorption data at a fixed 120 GHz, 61.9 GHz while illuminating the sample (thin films 150nm - 800nm thick) with 2 photon energy levels 266nm and 532nm, while the sample is exposed to very low (7K) to almost room temperature, and, also collecting the laser fluence (intensity) based millimeter wave (mmW) responses at each instance, and for each temperature regime. This structure-mmW property study was planned to be performed in the light of the field effect and high on/off current switching ability of these 3 materials of interest. We have been able to achieve substantially acquiring very high-quality temperature and laser fluence swept data set at 120GHz probe frequency using a tailor-made cryostat in the existing TR-mmWC apparatus and after calibrating the diode sensor of the cryostat. All the 3 material thin film samples were prepared as per literature and following best practices. However, we received mmW responses only for all the 4 different perovskite materials as planned. Based on the known structural changes of the perovskite material we have attempted to understand the mmW responses for the temperature-fluence datasets as much as possible. In this process, we have compared the new perovskite mmW responses to a 48,000-hour old perovskite sample that supposedly has age dependent recrystallization effects such as enhanced total lifetime, etc. We have compared the changes in biexponential decay time constants by age of the sample for the old sample in details. We have analyzed the step responses such as the 10-90% rise time, settling time, peak voltage and peak time from the averaged transients collected. Transmission coefficient and area of the curve have also been utilized to develop a successful sample age prediction model using the Gaussian Process Regression (GPR) technique. We have studied the variation of the biexponential fit coefficients (including the SRH and Auger time constants) with laser fluence for each of the 4 temperature regimes that the sample was exposed to. We have also presented results of the calculated mobility-carrier concentration product and how it varies with the calibrated cryostat temperature at each laser intensity on sample. The ratio of the slow to fast recombination (tail to peak ratio), and the ratio of positive to negative mmPCD peaks are also plotted as function of temperature, by each of the laser fluence level. Stem plots (3D) showing the mmW response as function of laser fluence (at each temperature) for the new (2022) perovskite samples one MAL3I and another CsPbBrI2 (inorganic) are also shown in the report. It is noted that 100K regime shows an increasing mmW response for the Cs-sample but, 150K is the regime that shows maximum of mmW response for the new MAL3I perovskite. It is also mentioned how we have attempted to prepare the new MAL3I sample using which we have obtained room temperature mmW response data and an X Ray diffraction pattern. We also present the problems faced with creating the PCB61M film and exposing to 50 keV electron beam for studying its band gap property. HfSe2 film was created not on a substrate but on Nitto tape affixed to a glass substrate. When we run TRmmWC, we can only note its dc property and transmission coefficient, but the mmW (radiofrequency) response is not able to be received. We will attempt one more time, hence, a collaboration has been started with the 2D crystal consortium at Penn State University recently, who will try to create an exfoliated sample using small crystals of HfSe2. This might possibly allow us to get good mmW responses. We have formed a very thin film on silicon for these materials and have only received AFM pictures of the flake (45nm tall) with surface roughness < 1nm and see the evolution of "bubbling" in the sample with age (in 48 minutes). For the future studies we believe that Field Effect Transistor (FET) analysis using the 3D form of the materials can be performed only after all the structural and millimeter-wave charge dynamical characteristics are acquired successfully. Here, we have progressed well in the direction of completing this project, but time limitations and resource management have been in the way of completing all the goals of this project in the specified time. In the future, we can carry on this work at least for the perovskite samples (through current small grant catalyst funding from NSF) produced using the proven techniques learned in the experimental phases to achieve results in this STIR project. However, a substantial set of TRmmWC response data collected for perovskites under sweeping temperature and laser fluence is a very important resource that was acquired through this STIR grant.

Most importantly, we have built confidence in using the cryostat-based mmW differential absorption data acquisition system mainly because we find the current technique to be very responsive to changes in laser fluence and temperature as well. We believe that, in the future, with this setup, it would be possible to acquire very high-quality structural-mmW property data by its functionality (such as field-effect) of novel semiconductors. We also plan to incorporate a suitable interferometer with the apparatus for the measurement of the dielectric property of the material at every probe frequency, and, also, will attempt to measure, and acquire structural changes radiative decay signals while the experiment is implemented.

Training Opportunities: One graduate student of physics was trained on use of the TRmmWC apparatus to work with the cryostat and on data acquisition and analysis.

Results Dissemination: Nothing to Report

RPPR Final Report
as of 11-Apr-2023

Honors and Awards: Nothing to Report

Protocol Activity Status:

Technology Transfer: Nothing to Report

PARTICIPANTS:

Participant Type: Faculty
Participant: Marvin H Wu
Person Months Worked: 9.00 **Funding Support:**
Project Contribution:
National Academy Member: N

ARTICLES:

Publication Type: Journal Article Peer Reviewed: N **Publication Status:** 0-Other
Journal: arXiv
Publication Identifier Type: DOI Publication Identifier: 10.48550/arXiv.2211.02431
Volume: v1 Issue: First Page #:
Date Submitted: 1/6/23 12:00AM Date Published: 11/4/22 4:00AM
Publication Location: Cornell University, Ithaca, New York
Article Title: Supervised learning applied to high-dimensional millimeter wave transient absorption data for age prediction of perovskite thin film
Authors: Biswadev Roy*, Abdennaceur Karoui, Branislav Vlahovic, and Marvin H. Wu
Keywords: perovskite, photoconductive-decay, recombination, millimeter-wave, aging
Abstract: We have analyzed a limited sample set of 120 GHz, and 150 GHz time-resolved millimeter wave (mmW) photoconductive decay (mmPCD) signals of 300 nm thick air-stable encapsulated perovskite film (methyl-ammonium lead halide) excited using a pulsed 532-nm laser with fluence 10.6 µJ cm-2. We correlated 12 parameters derived directly from acquired mmPCD kinetic-trace data and its step-response, each with the sample-age based on the date of the experiment. Five parameters with a high negative correlation with sample age were finally selected as predictors in the Gaussian Process Regression (GPR) machine learning model for prediction of the age of the sample. The effects of aging (between 0 and 40,000 hours after film production) are quantified mainly in terms of a shift in peak voltage, the response ratio (conductance parameter), loss-compensated transmission coefficient, and the radiofrequency (RF) area of the transient itself (flux). Changes in the other step-response parameters and the
Distribution Statement: 2-Distribution Limited to U.S. Government agencies only; report contains proprietary info
Acknowledged Federal Support: **Y**

RPPR Final Report
as of 11-Apr-2023

Publication Type: Journal Article Peer Reviewed: Y **Publication Status:** 4-Under Review
Journal: Materials Letters
Publication Identifier Type: Other Publication Identifier: MLBLUE-D-23-00887
Volume: Issue: First Page #:
Date Submitted: Date Published:
Publication Location:
Article Title: Facile Synthesis and Morphology-Induced Photo-conductivity Modulation of Bi2O2S Nanostructures
Authors: Basant Chitara, Biswadev Roy, Marvin H. Wu, and Fei Yan
Keywords: Solution-processing; Bi2O2S nanostructures; Transient photoconductivity; HH
Abstract: This study presents the time-dependent photoconductivity behavior of layered Bi2O2S semiconductor nanostructures, which are synthesized via solution processing at room temperature, with or without the inclusion of hydrazine hydrate (HH) as a modifying agent. The results reveal that the addition of HH during the synthesis produces thinner nanostructures with faster carrier trapping times due to surface defects, while the bulk trapping and recombination times remain similar. The longer rise time in both samples may indicate enhanced exciton binding energies resulting from confinement to two dimensions. The research highlights a promising approach to modulate the transient photoconductivity of layered semiconducting materials by introducing varying amounts of reducing agents during the bottom-up synthesis.
Distribution Statement: 2-Distribution Limited to U.S. Government agencies only; report contains proprietary info
Acknowledged Federal Support: **Y**

Publication Type: Journal Article Peer Reviewed: N **Publication Status:** 0-Other
Journal: TechrXiv
Publication Identifier Type: DOI Publication Identifier: https://doi.org/10.36227/techrxiv.22082360.v
Volume: Issue: First Page #:
Date Submitted: Date Published: 2/15/23 5:02PM
Publication Location:
Article Title: Comparison of time-resolved millimeter-wave responses between aged and new perovskite thin films
Authors: B. Roy, J. Chai, R. Su, F. So, and M.H. Wu
Keywords: time-resolved, millimeter wave, perovskite, transmission, reflection.
Abstract: To develop structure-microwave property relationships of novel perovskite material which demonstrate room temperature super-fluorescence properties we have first discussed the changes in time constants of photo decay transients at 150 and 120 GHz for an aging hybrid perovskite (methyl ammonium lead halide, MAPbI3) sample for the first 10,000 hours, and then compared the 120 GHz time-resolved millimeter-wave (mmW) conductivity responses and performances of a 47,000-hour old hybrid perovskite, with responses of 2 new 200-300 nm thick films one, hybrid MAPbI3, and another inorganic CsPbI2Br perovskite film at room temperature. We find that with the 150 GHz probing, the time constant for 1-, 2- and 3-exponential decay fits show a significant departure with sample age. The new and old MaPbI3 films both display a better lifetime in reflection mode, but, in general, surface reflection signals offer the best lifetimes for 10.6 μJ cm-2 laser fluence.
Distribution Statement: 2-Distribution Limited to U.S. Government agencies only; report contains proprietary info
Acknowledged Federal Support: **Y**

RPPR Final Report
as of 11-Apr-2023

Partners

,

I certify that the information in the report is complete and accurate:
Signature: Biswadev Roy
Signature Date: 4/10/23 4:54PM

FINAL REPORT

- Federal Agency and Organization Element to Which the Report is Submitted

  U.S. Army contracting command – Aberdeen Proving ground – Research Triangle Park Division (ACC-APG-RTP Division)

- Federal Grant or Other Identifying Number Assigned by Agency

  Army Research Office Award Number W911NF-22-1-0116

- Project Title

  Structure-property relationships of novel electronic functional materials using contactless probing

- Project Director/Principal Investigator (PD/PI) Name, Title, and Contact Information (e-mail
  - address and phone number)

Dr. Biswadev Roy
Research professor,
#1159 Microwave materials characterization laboratory
Mary Townes Science Complex
1900 Concord St., Durham, N.C. 27707
broy@nccu.edu
(919) 530-6350 (work)
(919) 599-2043 (mobile)

- Name of Submitting Official, Title, and Contact Information (e-mail address and phone
  - number), if other than PD/PI **(not applicable)**
- Submission Date

  March 30, 2023

- DUNS and EIN Numbers

  DUN and Bradstreet (DUNS): 783691801, UEI: L1DXXP1KGP77
  Employer Identification Number (EIN): 56-6000730

- Recipient Organization (Name and Address)

  North Carolina Central University
  1801 Fayetteville St.
  Durham, NC 27707-3129

- Recipient Identifying Number or Account Number, if any

  Fund Number: 556180
  IPF Number: 22-0109

- Project/Grant Period (Start Date, End Date)

  Start Date: July 01, 2022
  End Date: March 31, 2023

- Reporting Period End Date

  March 31, 2023

- Report Term or Frequency (annual, semi-annual, quarterly, other)

  Final Report for STIR grant

- Final Report?

  Yes

- Signature of Submitting Official (signature shall be submitted in accordance with agency specific instructions)

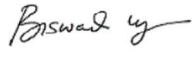

(Biswadev Roy)

Abstract: Field effect transistor (FET) is an important robust 3-terminal device. Conventional FETs are made of silicon and are used widely in electronics and communication systems. We wanted to study 3 types of novel materials that possess exciting optoelectronic properties and wide use in solar photovoltaic energy conversion and also show excellent current switching on/off ratio, and strong field-effect capabilities. For this, we selected 3 different types of new materials one hybrid (crystal-molecular) perovskite (methyl ammonium lead iodide, samples P1, P2, and P4), an inorganic perovskite ($CsPbBrI_2$, sample P3), one band gap tunable methanofullerene [6,6]-phenyl C_{61}-butyric acid methyl ester (PCBM), and one high mobility and large work function small band gap transition metal dichalcogenide (TMD) hafnium Di selenide (hfSe2). We want to establish structure-microwave charge dynamical property relationships by experimental evaluation of each of the types of samples by using thin films (2D), once for the natural aging of the sample and another time, subjecting the samples to temperatures in the range 340K-7K. In solar cells, the charge is transported vertically within 100s of nm thick grains but, in planar FETs, transport occurs laterally. However, using the contactless microwave absorption technique we can sample the 3D volume that makes up the probe beam cross-section area extending up to the light penetration depth. This control volume is of interest and should provide enough charge transport property information to infer the field effects that would be exhibited by the 3D film of the material itself. We have completed a major part of the goals. We have prepared thin film samples of each different type of material and its variety as per literature and calibrated a cryocooler after adding it successfully to the existing TR-mmWC apparatus. 47,000-hour old and new MA Perovskite samples are compared in terms of their decay time constants using 1-, 2- and 3-exponential fits. The ratio of Auger- to SRH recombination process lifetime is found to be 0.09 and SRH lifetimes are laser fluence invariant. The lifetime differences between the new and old samples increase with time. Simultaneous transmission and reflection signals of the old and new P3 perovskites signify that the carrier concentration-mobility product (transmission/reflection) bears a ratio of 6.5 and for perovskites P2, and P1, the ratio is 4.3 and 4.8 respectively. It is found that age-correlated step responses can be used in a machine learning model for age prediction. This technique is a success. After applying Savitsky-Golay filtering to the averaged transients and considering the background noise, it is possible to get a very good temperature and laser fluence swept TRmmWC response datasets. The response itself shows two transition temperatures at all laser fluence levels, viz. 55.2K and 151.5K and the carrier concentration-mobility product decreases with temperature with a slope of ~0.2. The ratio of slow- to fast decay coefficients (time constants) shows an interesting increase with temperature when fluence is at 1.4 $\mu J\ cm^{-2}$. Positive to negative peak voltage ratios show most peaks accruing at moderate temperatures but, at lower fluences only. The 10%-90% rise time (an inherent resistive-capacitive property) shows variation with age, and temperature. A thick sample of Hafnium Di selenide provided a very good TRmmWC response at 266nm laser with a meager $5\mu J\ cm^{-2}$ laser fluence. The sample P4 on sapphire substrate yields a very promising transmission coefficient (0.98, compared to other perovskites on glass). PCBM sample was built but could not be lasted due to its destruction by acetone used in the process of putting a mask on to the film that was being prepared for electron beam irradiation for the supply of $13{,}000\mu C/cm^2$ charge to see if the band gaps are altered. This experiment will be repeated and, a new 300nm $HfSe_2$ sample is being prepared by the 2D Crystal Consortium (2DCC) at Penn State University which is self-funded. We believe we could get a good set of TRmmWC responses out of these.

What were the major goals and objectives of this project?

- To establish structure-property-field effect relationships of three different materials viz. indirect band gap hybrid methyl-ammonium lead iodide (MAL3I) with a perovskite structure having indirect band gap ~1.5 eV, a slightly n-type indirect band gap (~1.1eV) Hafnium di-selenide (a transition metal dichalcogenide), and a purely organic acceptor material [6,6]-phenyl-C 61 - butyric acid methyl ester (PCBM) and its electron beam irradiated variant, with optimal band gap 1.3-1.9 eV by subjecting various samples to different temperatures using a well-calibrated cryostat.
- The goals for the MAL3I investigation involve A) how specimen combined Wannier-Mott and Frenkel excitons behave in terms of the changes in external temperature of the sample (influence of spin-orbit coupling and its effect on mobility measured at millimeter wave probe frequencies) for the temperature range 8K-350K and also by age of the sample. B) What is the signal settling time when voltage response and their steady-state differences are ~2% of the peak voltages and how does the positive- to negative photo response voltages behave for studying the extents of sloe- and fast recombination process, C) Whether the shallow trap developments aid in enhancing lifetime as observed at millimeter wave frequencies and does chemical passivation of MAL3I have any pronounced effect on the shape of the conductance kinetics (charge population relationship with mobility). D) To include the structural information from MAL3I investigations to study photo responses.
- The goals of fast switching material group IV TMD Hafnium di-selenide thin film include A) obtaining structural information from the Raman system and SNOM, B) generating averaged photo-transients using millimeter wave pump-probe spectroscopy (TR-mmWC) and study variation of peak voltages with age and structural changes induced due to external temperature, and use the crystals to create test chips for FET measurements and its relationships with the structural changes and millimeter wave response.
- Goals of 99.5% pure electron acceptor material PCBM (Methanofullerene [6,6] – phenyl C61-butyric-acid methyl ester) include: A) studying photo responses using 266nm laser induced millimeter wave probed charge carrier dynamics also at external temperatures 8K-350K. B) to study the effect of 50 keV/1.6 μA electron beam irradiation on 99.5% pure PCBM film on its band structure (effect of alteration of the lowest unoccupied molecular orbital level by electron beam)

The overall objective of the project was to relate the structure of 3 different types of semiconductor thin films viz. aged, and new MAL3I: a hybrid thin film, a $CsPbI_2Br$ (perovskite structure, but completely inorganic constitution), a $HfSe_2$ inorganic thin film and PCBM, a purely organic thin film using noise-free averaged transient datasets obtained from using the in-house time-resolved millimeter wave conductivity apparatus in transmission and reflection mode, and, finally relate to their respective field-effect functionality merits for justifying its use as a reliable Field Effect Transistor (FET) material.

What was accomplished under these goals?

1. Results for Perovskite samples

1.1 Sample preparation

Three MAL3I thin films and one $CsPbBrI_2$ film (all with perovskite structure) were spin-coated on glass/sapphire and then DC and radiofrequency (RF) characterized in a contactless method using 0.34mW fixed 120 GHz probe in a quasi-optical setup while the thin films were subjected to temperatures in the range 300K to 7K (to measure mmW response signals off the *cubic-tetragonal-orthorhombic* structures in each of the temperature regimes) using a well-calibrated cryostat attached to the time-resolved millimeter wave conductivity apparatus[1]. All MAL3I thin films are direct band gap

semiconductors (with some literature pointing its direct-indirect character), $CsPbBrI_3$ is a direct wide band gap material whereas $HfSe_2$ is a slightly n-type indirect bandgap material. We will name the perovskite samples by numbers 1, 2, 3, and 4 abbreviated as **P1, P2, P3, and P4.** The samples P1, P2, and P4 are variants of MAL3I (all with hybrid structure)[2-6] and P3 is an inorganic perovskite $CsPbBrI_2$.[7] The thicknesses of P1, P2, P3, and P4 are 300-350nm, 285nm, 150nm, and 800nm respectively. P1 was spin-coated on a quartz substrate, P2, and P3 were spin-coated on glass[8] using precursors at the North Carolina State University (NCSU) materials science department and P4 was spin-coated on sapphire at the Shared Materials Instrumentation Facility (SMiF) at Duke University. Sample P1 was prepared in the year 2017 and most of the aging studies have been performed for its ages between 0 and 40,000 hours. At the time of acquiring cryostat-based temperature responses in millimeter wave probing, the sample age was precisely 48,720 hours from the time of its production. Sample P1 precursor was prepared by first dissolving PbI_2 in dimethylformamide at a concentration of 800 mg mL^{-1} and then spin coating on a 1 mm thick quartz glass substrate at 2000 RPM for the 60s. Methylammonium iodide (MAI) was then dissolved in isopropanol at a concentration of 95 mg mL^{-1} and the solution was subsequently spin-coated on the PbI2 surface at 6000 RPM for the 30s. These films were then annealed at 100°C for 2 hours. Sample P1 was then encapsulated using glass glued with epoxy for protection from humidity and other air contaminants. Sample P2 was prepared also at NC State University using the precursor solution by dissolving PbI_2 (99.999%), Methyl Ammonium Iodide (MAI), and dimethyl sulfoxide (DMSO) at a molar ratio of 1:1:1 in dimethylformamide (DMF) at a concentration of 1M and then spin-coated on the glass substrate, during which 100µl of toluene was dropped on the sample at the 8th second. The film was then annealed at 100°C for 10 minutes to complete the crystallization process. Sample P3 ($CsPbBrI_2$) was made[9] by mixing 0.3m $CsPbI_3$ and 0.3M $CsPbBr_3$ in the ratio 2:1 and then spin-coated on a glass substrate at 3000 RPM for 1 min. followed by an annealing process for 8 min. at 85°C. Sample P4 was produced using MAL3I precursor solution obtained from Osilla, Ltd. (U.K.) and spin coating on sapphire substrate spun at 3000 RPM with a ramp-up of 200/s, and then, annealed the film for 10 minutes at 100°C.

1.2 Cryostat calibration

A closed cycle DE-202 compact cryocooler (Applied Research Systems make) was assembled into the TRmmWC set up to act as cryostat in which, the sample housing was equipped with sapphire windows on each side and a central holding frame where the sample was attached with one 1N4148 diode was used as the temperature sensor. This diode was calibrated using a reference Omega Pt-based resistance temperature detector (RTD) temperature was measured manually by cooling it in a helium bath and heating the sensor using hot air flow from a heater while the diode and RTD sensors were tightly connected and held at the same location while the diode temperature was registered by a Lakeshore 331 controller. The cryostat calibration chart was drawn (as shown in Figure 1) and a linear regression was used to correct all diode-derived temperatures that were subsequently registered by the Lakeshore 331 controller. The calibration chart is shown in Fig. 1. In subsequent experiments conducted with P1, P2, P3, and P4, the cryostat was placed in an ultra-high vacuum (~ 10^{-4} Torr) using a Pfeiffer Hi cube 80 eco vacuum system and an ARS-4 HW helium compressor with 2 helium hoses was used for achieving cooling cycles to subject the perovskite samples to temperatures as low as 7K.

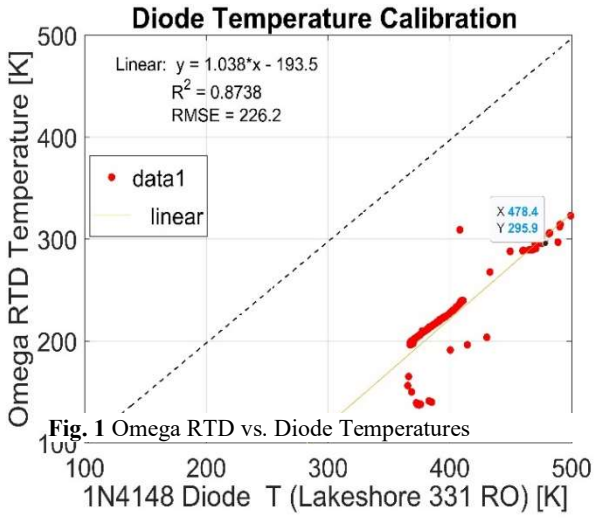

Fig. 1 Omega RTD vs. Diode Temperatures

1.3 Results on comparing millimeter wave responses between aged sample (P1) and new samples (P2, P3) without a hole transport layer.

To develop structure-microwave property relationships of novel perovskite material the changes in time constants of photo decay transients at 150 and 120 GHz for an aging hybrid perovskite (methyl ammonium lead halide, $MAPbI_3$) sample made in the year 2017 for the first 10,000 hours are analyzed. A comparison of 120, and 150 GHz millimeter-wave (mmW) conductivity (TR-mmWC) responses and performances of then 47,000-hour old hybrid perovskite, are made using mmW responses of 2 new 200-300 nm thick films one, hybrid MAPbI3, and another inorganic $CsPbBrI_2$ perovskite film (both made in August 2022) at room temperature. TR-mmWC signal is sensitive to differential absorption of the mmW probe beam due to apparent change in electron population changes in the sample when light is incident on a sample at enough energies to surpass the band gap. It is found that with the 150 GHz probing, the time constant for 1-, 2- and 3-exponential decay fits show a significant departure with sample age. The new and old $MaPbI_3$ films both display a better life in reflection mode, but, in general, surface reflection signals offer the best lifetimes for 10.6 μJ cm^{-2} laser fluence.

1.3(a) mmW photo decay experiment & data acquisition

The 120 GHz data were obtained using probe signals from an impact ionization avalanche transit-time (IMPATT) diode oscillator and 150 GHz data are obtained using a specialized vacuum tube oscillator. The system is quasi-optical because the wavelength is ~2.5 mm which is comparable to the size of the optical elements in the experimental path. This pump-probe uses a 532 nm laser pump with a pulse width of fewer than 0.69 ns and is pulsed 1 kHz, thereby offering enough sensitivity to acquire mmW transients with a time resolution of around 100 ps with a minimum detectable photoconductance ~1 μSiemens. Fig.2 shows the optics arrangement.

In the case of the perpetually aging perovskite sample, we use a full laser fluence ~10.6 μJ cm^{-2} with pulsed energy around 20 μJ to excite the sample with a laser spot area of ~87 mm^2 and the continuous wave (CW) mmW probe beam with a diameter of ~6.2 mm^2 diodes and low-noise amplifiers whose gains are 31.48 dB and 31.82 dB for the transmission and reflection lines respectively, and the corresponding Schottky diodes bear responsivity of 1600 V/W and 3600 V/W respectively. Less than 0.5 mW of mmW probe power is incident on the sample at any given time.

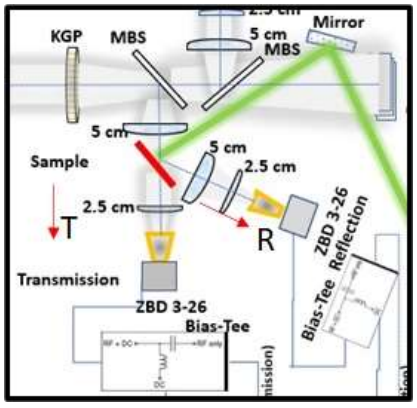

Fig. 2 TR-mmWC simultaneous transmission-reflection setup. KGP: Polarizer, MBS: Splitter, ZBD: Detector

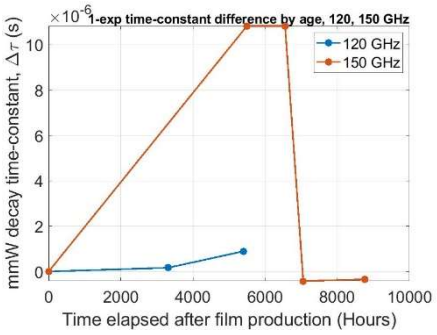

Fig. 3 Differences in time-constant for 1 exp fits

1.3(b) mmW decay time constant (3-exp fit) changes between 0-10,000 hours

It is seen that with 150 GHz probing of the aged sample, the mmW decay signal exhibits a steady decline of 10%-90% rise time, the peak voltage settling time, and the peak time to lower values with sample age. Both are indicative of the formation over time of recombination centers in the material. A significant change is observed at about 7000 hours. The observed dynamics through the mmW decay allow an understanding of the type of formed recombination center. To that end, we have extracted the time constants (τ) for single exponential: a*exp(-t/τ) and plotted the differences (Δτ) shown in Fig.3, for 2-exponential: b*exp(-t/τ_1) + c*exp(-t/τ_2) shown in Fig. 4, and for the 3 exponential recombination lifetimes: d*exp(-t/τ_3) + e*exp(-t/τ_4) + f*exp(-t/τ_5) separately from the obtained mmW decay signals in Fig. 5. These data include the 150 GHz acquired mmW decay signals (5 experiments performed on different dates) and the 120 GHz observations (at three different dates). It is important to attribute the various lifetimes each to one mechanism (fast and slow recombination) as well as the localization of the recombination centers, surface versus bulk. Figure 5 shows the variation of the time constants by sample age for the first 10,000 hours.

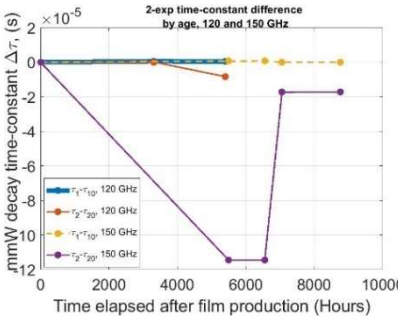

Fig. 4 Tau-1 and Tau-2 differences for 2-exp fits

The differences in recombination carrier lifetimes τ (obtained from the mmW decay time constants) are noted when the time constants of the sample are plotted as a function of its age (in hours). The average Auger to Shockley-Read-Hall (SRH) lifetimes ratio for the 120 GHz and 150 GHz (combined data) is found to be 0.09 In non-radiative recombination Auger processes have shorter periods than the trap-assisted SRH recombination. Also, SRH time constants are mostly invariable with laser fluence. The 120 GHz lifetime differences (Δτ) between the pure sample and the aged sample for single, double, and 3 exponential decays, all increase with time, and are remarkably higher after 3400 hours. For the 150 GHz signal, we note that the Δτ has a consistent decreasing tendency with the age of the sample. A notable change in 1-exp, 2-exp, and 3-exp Δτ is observed around 7000 elapsed hours.[10]

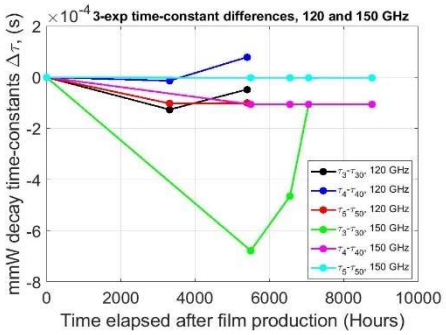

Fig. 5 Rad., SRH and Auger time constant differences from original signal from 3-exp fits

1.3(c) Comparison of perovskite response at 47,000 hours with 2 new perovskite films

The mmW response ratio ($\Delta V_{RF}/V_{dc}$) profile obtained for the 2 new perovskites (2022) samples are plotted together in one, for a direct comparison of the photoconductance property (actually the ratio directly provides the carrier-concentration-mobility product) obtained simultaneously from transmission (T) and reflection (R) data. Figure 6 shows the plot of the responses. During a previous study, it is noted that few of the TR-mmWC signal characteristics bear a very strong negative correlation with the sample age and those parameters can be used to predict the sample age with very strong confidence. While using the T-R signals the magnitudes of 4 of the step response parameters are used for establishing a machine learning (ML) model to predict the age of the

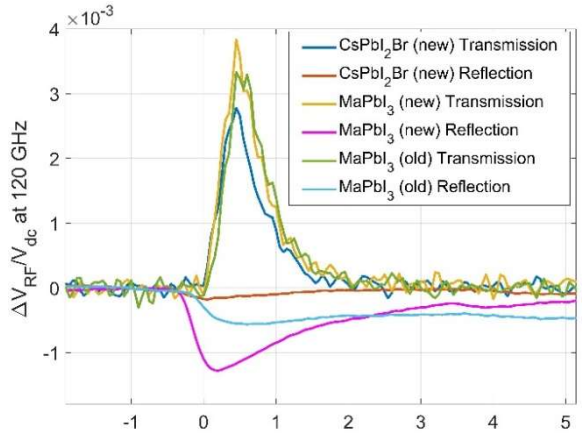

Fig. 6 TR-mmWC Transm.-Refl. Response ratio $\Delta V/V_{dc}$.

sample. The most negatively correlated parameters (with sample age) are given in Table I below. This study[11] reveals the following characteristics:

Room temperature differential absorption data sets from one aging (the year 2017) perovskite $MaPbI_3$ sample have shown the following:

- 10%-90% signal rise time, peak settling time, and peak voltage, all decrease with the age of the sample.
- Auger to SRH lifetime ratio is found to be 0.09 using the 3-exponential fitting.
- The 150 GHz 3-exponential fit shows that the Auger lifetime bears maximum departure with the age of the sample(τ_5).
- Hybrid $MaPbI_3$ shows better photoconductivity response both, for transmission mode as well as surface-based reflection mode at 120 GHz.
- Hybrid perovskite (both, old and new samples) exhibit a good decay period in surface reflection mode.
- The transmission-based carrier concentration-mobility product to its reflection-based product ratio bears 6.5 in the case of inorganic perovskite $CsPbBrI_2$ whereas both the hybrid $MAPbI_3$ (new and old) bears a ratio of 4.3 and 4.8 respectively.

Table I: Magnitudes of 4 TR-mmWC strong negatively correlated parameters with sample age

Sample	T_{decay} (s)	mmW response $\Delta V_{RF}/V_{dc}$	Transm. Coeff./Reflection Coeff. (%)	$\int V(t)dt$, Wb.
$CsPbBrI_2$				
Transmission	2.5e-09	0.0028	40.42	1.064e-13
Reflection	2.7e-09	6.5e-04	65.15	3.002e-14
$MaPbI_3$ (new)				
Transmission	2.60e-09	0.0038	31.01	6.85e-13
Reflection	Very long	0.0013	61.02	4.36e-13
$MaPbI_3$ (old)				
Transmission	2.8e-09	0.0033	17.44	4.17e-13
Reflection	Very long	6.3e-04	87.96	3.24e-12

Hence, it will be useful to look at the temperature dependence of these parameters using perovskite samples without a hole transport layer. This is important because the dielectric constant of the material will change with probe frequency and temperature as well. This will reveal a complete picture of the non-radiative decay processes in these novel materials.

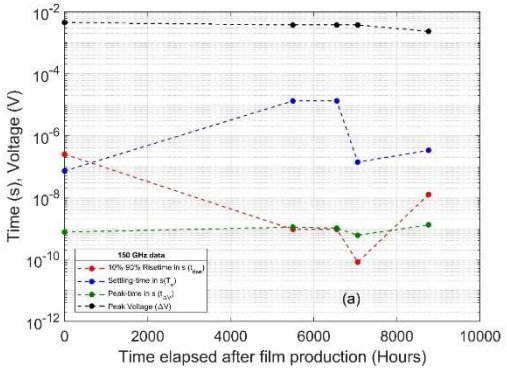

Fig. 7 Shows 4 step-responses extracted from averaged 150 GHz kinetic trace between 0-10,000 hours

1.4 General results on changes in step-responses and transmission coefficient by age[10] of perovskite sample P1

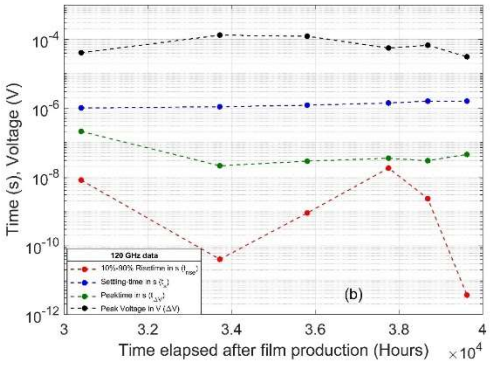

Fig. 8 Same as in Fig.7 but for sample ages between 10,000-40,000 hours

Considering the millimeter wave photoconductive decay (mmPCD) signal analogous to a single input, single output (SISO) continuous, time-invariant dynamic system and the size of the response vector (ΔV) is acquired with the same number of delay in seconds after the laser is turned off. The decay begins just following the settling maximum voltage, we plot the 4 important directly acquired step-responses by respective

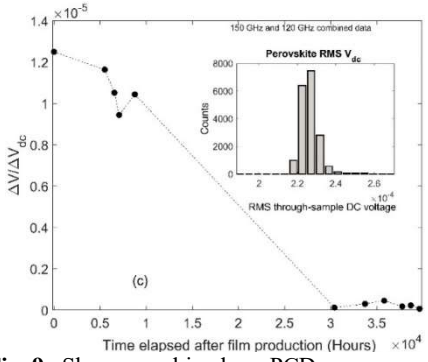

Fig. 9 Shows combined mmPCD response ratio with age of sample; Inset: histogram of RMS DC value (no

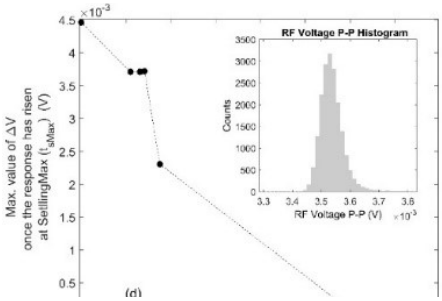

Fig. 10 Max. values of the peak when response rose to t_sMax; Inset: histogram of RF peak-to-peak voltages for one session

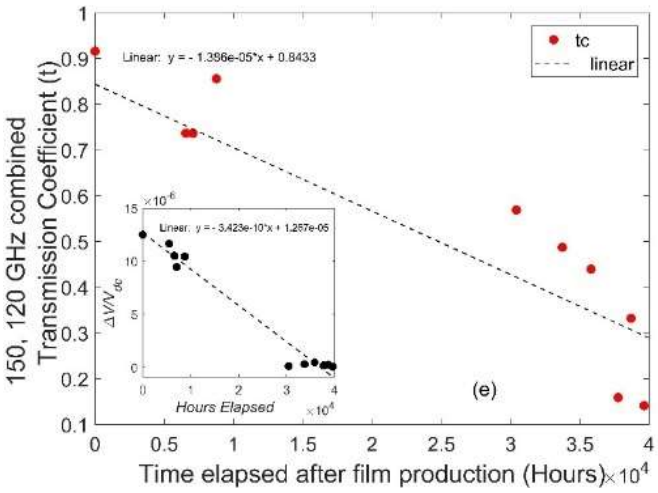

Fig. 11 Shows transmission coefficient of MAL3I film by its age in hours; Inset: mmW response as function of sample age.

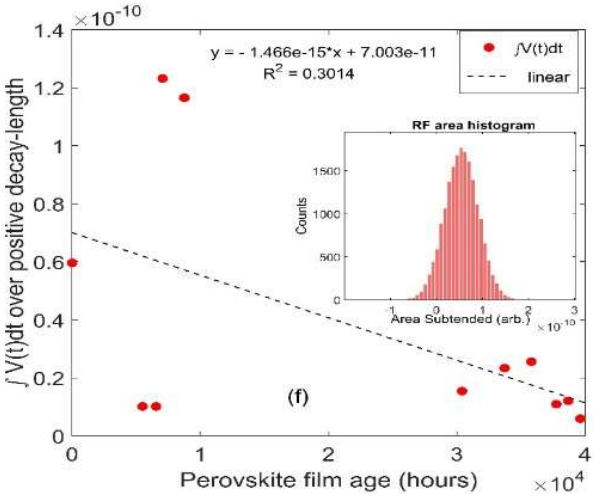

Fig. 12 Voltage-time product for 11 unique dates data were collected, as function of sample age in hours; Inset: histogram of one of the areas for one session obtained without voltage bias correction.

sample-age, to note additional behavior of material property and their effects. The directly obtained step response data considered in Gaussian Process Regression (GPR) model[11] are, the signal 10%-90% rise-time (t_{rise}), representing the intermediate carrier concentration states when the sample is excited by the laser before achieving the full level of photoconductance. The rise-time is also representative of the apparent capacitive-resistive state of the material as it ages over time. We anticipate a change in the rise-time due to the aging process. The settling time (t_s) is analogous to the recombination period of the signal, except for the fact that this is the time it takes to achieve the response reaching 2% of the peak voltage (ΔV) achieved at the peak time. Peak time ($t_{\Delta V}$) in seconds is the only step response that shows a positive correlation with perovskite sample age in hours. Figures 7 and 8 show these four-step responses as a function of sample age in hours acquired at 150 GHz and 120 GHz respectively. Two additional datasets are included while plotting the 120 GHz data shown in Figs. 7 and 8 considering 10/01/2021, and 11/09/2021 data with time elapsed after film production at 38,688 hours and 39,624 hours respectively. It is readily noted that the t_{rise} is the most varying step-response at both the probe frequencies and, in general, the baseline rise-time at 150 GHz at ages between 0 and 10,000 hours is longer than those obtained at 120 GHz at ages between 30,000 and 40,000 hours. Figures 9 and 10 show variations of TRmmWC response ratio and r_{ise} with age. Figure 11 shows the variation of 150, and 120 GHz transmission coefficient changes with sample age with an inset showing the TRmmWC response ratio (a measure of carrier conc.-mobility product) with age, and Figure 12 shows the age variation of the voltage-time area of the transient itself.

1.5 Results on the behavior of temperature, and laser fluence dependent bi-exponential coefficients of the aged perovskite thin film sample P1

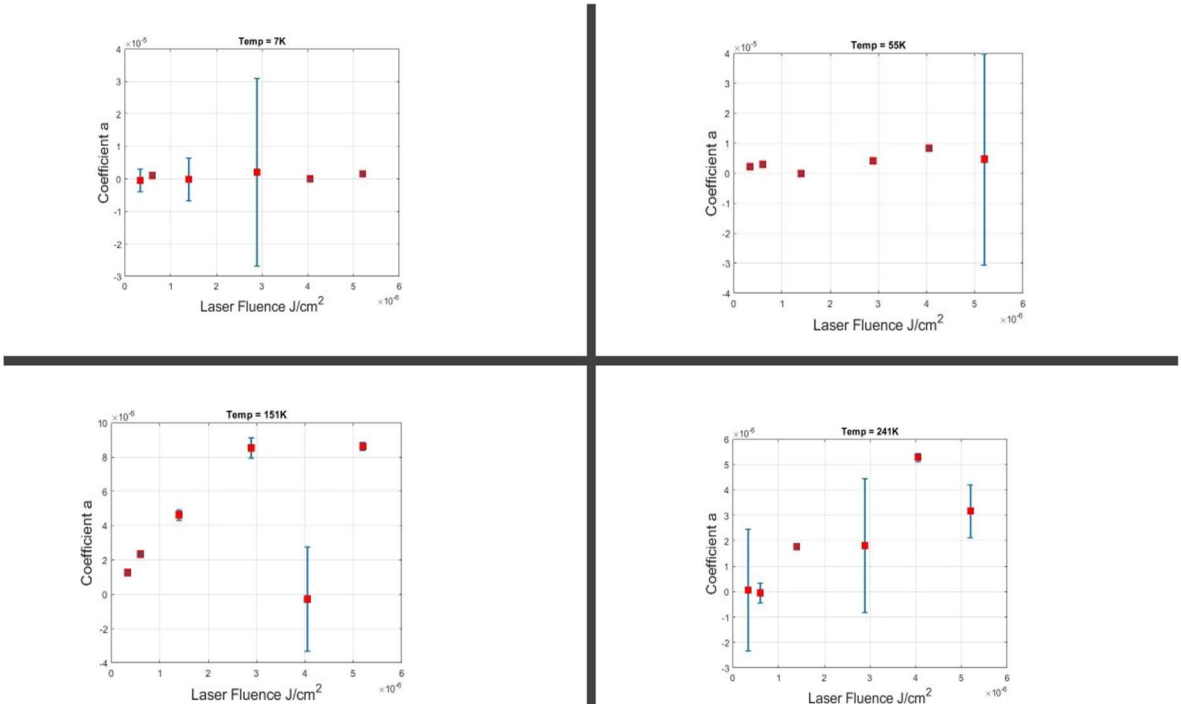

Fig. 13 Variation of bi-exp coefficient 'a' with laser fluence at 4 cryostat temps for sample P1. The margins of error for each instance.

To study the effect of temperature and laser fluence on the mmW response of the aging perovskite sample, we have considered studying the bi-exponential fit coefficients described by $a*\exp(-t/\tau_1) + b*\exp(-t/\tau_2)$ as described earlier. This analysis revealed the general characteristics of the sample responses based on non-radiative losses arising due to defects in the crystal-molecular levels. These properties will prove to be useful for studying[13] the structure-property relationship from the carrier concentration and mobility point of view. Figures 13 (above) show the variation of the bi-exponential fit coefficient, 'a' with laser fluence in Joules/cm^2 for each of the cryostat temperature regimes viz. 7K, 55K, 151K and at 241K. Figures 14, 15, and 16 show the variation of τ_1, Coefficient 'b', and the time constant τ_2 respectively. All temperature and laser-swept data sets have been passed through a well-designed Savitzky-Golay filter (7th order, with a frame length of 999). The background signal is collected after averaging the same number of times as the main mmPCD signal but, without any laser activity, and placing the material in the path of the probe signal. This background is also Savitzky-Golay filtered before subtracting from the main signal obtained while laser illumination of the sample

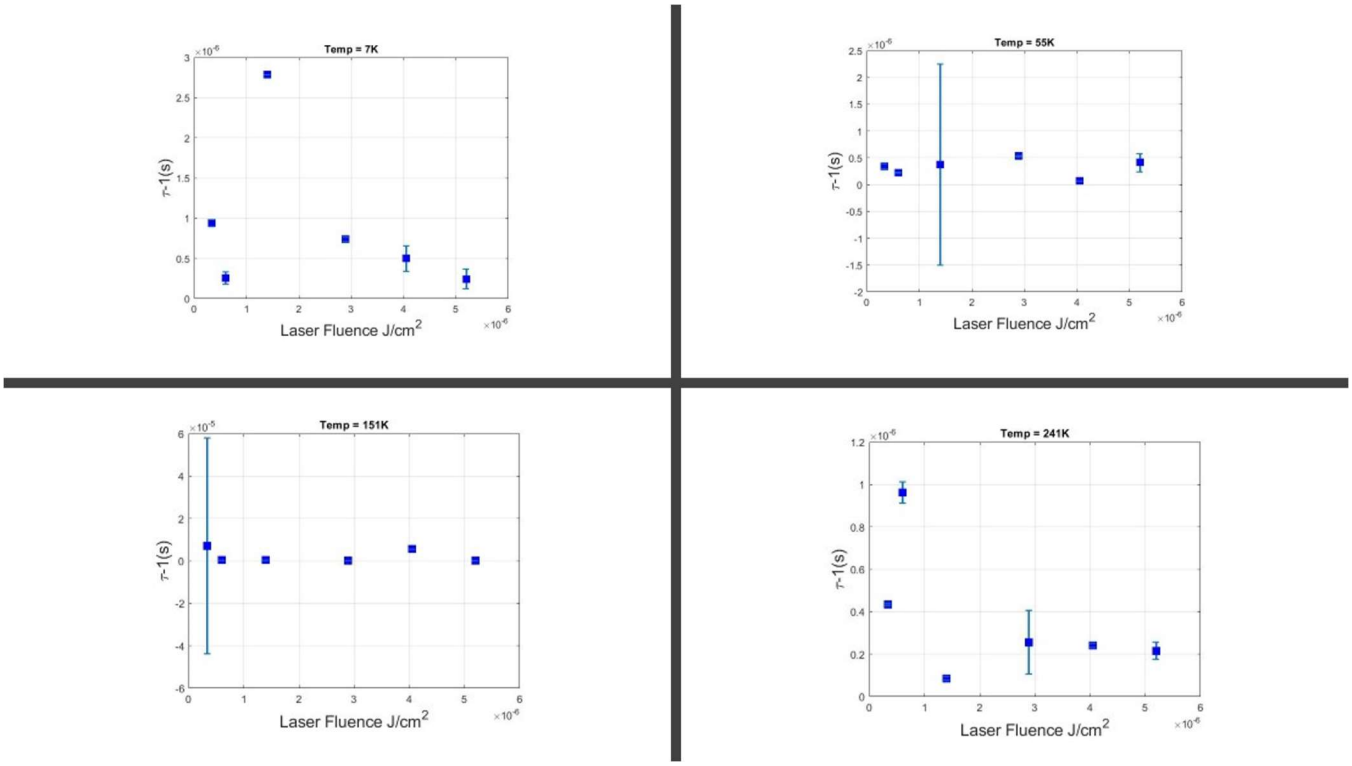

Fig. 14 Variation of bi-exp time constant 'τ_1' with laser fluence at 4 cryostat temps for sample P1. The margins of error for each instance.

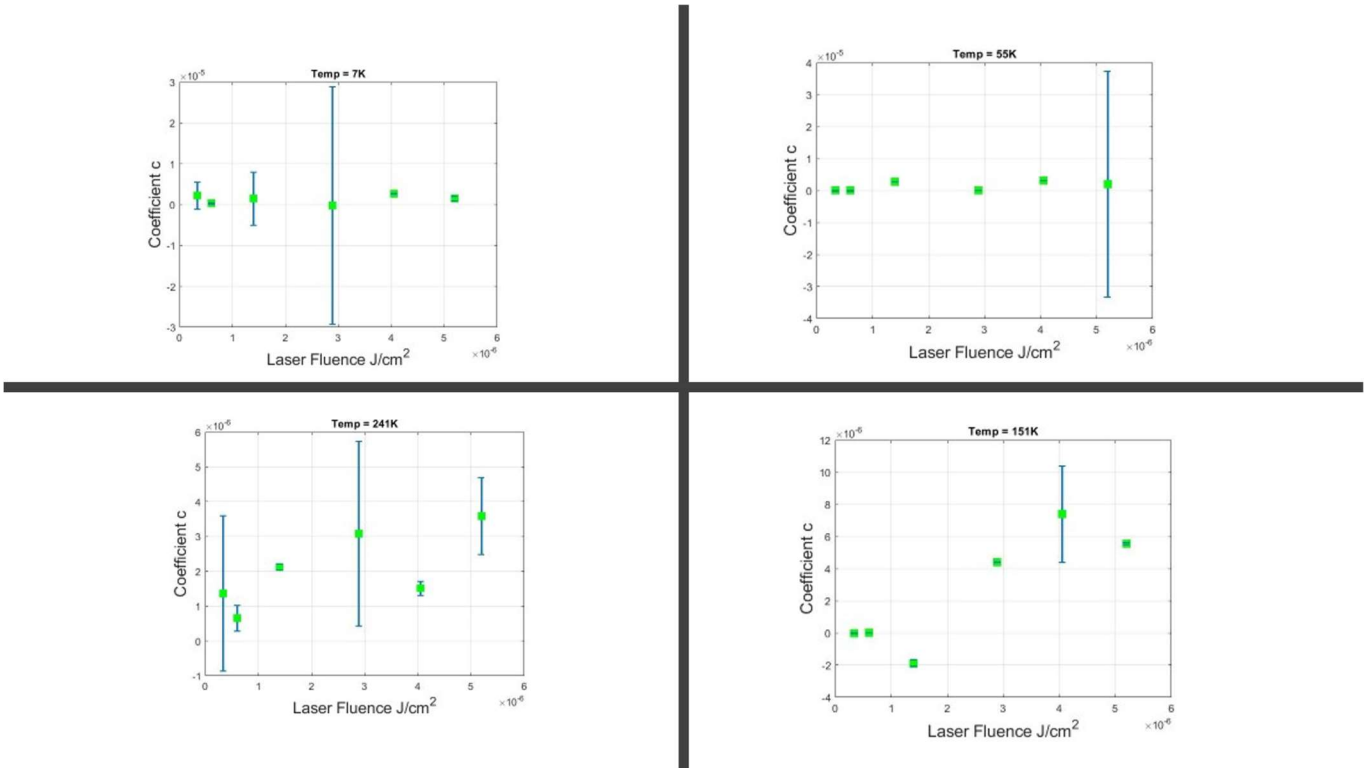

Fig. 15 Variation of bi-exp coefficient 'b' with laser fluence at 4 cryostat temps for sample P1. The margins of error for each instance.

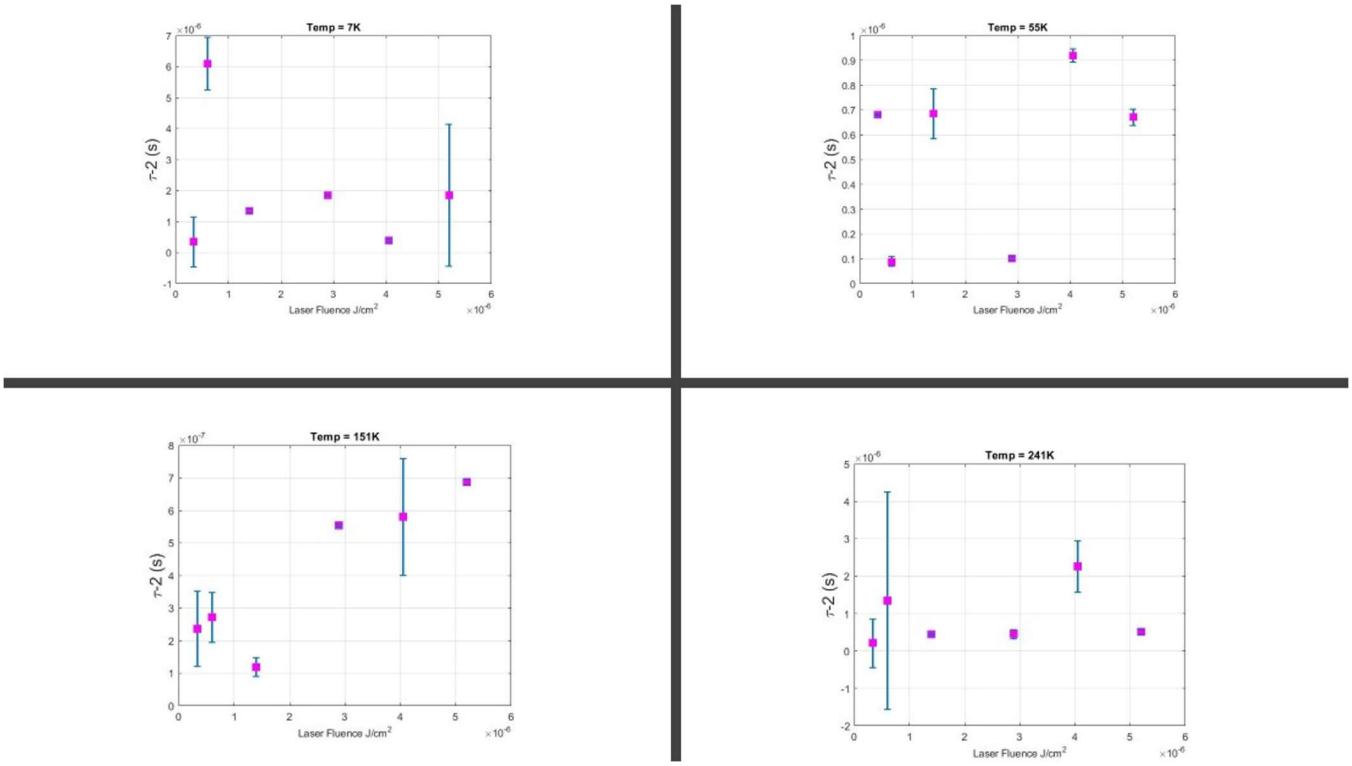

Fig. 16 Variation of bi-exp time constant 'τ_2' with laser fluence at 4 cryostat temps for sample P1. The margins of error for each instance.

Similar variation plots for the other samples P2 and P3 are also done but not shown here. We will

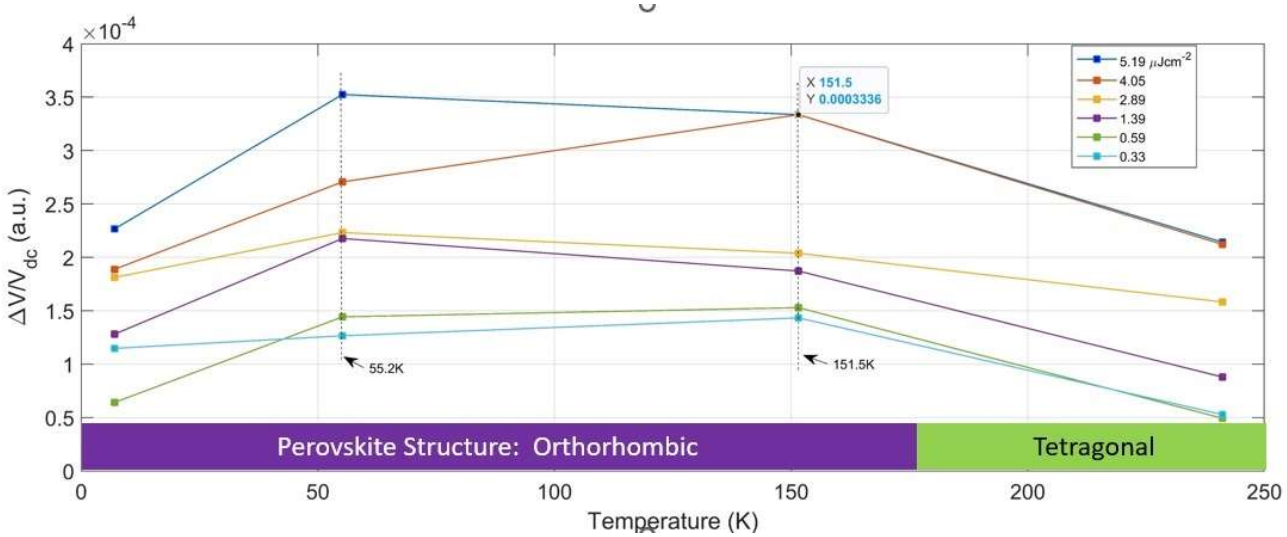

Fig. 17 Variation of TR-mmWC gain $\Delta V/V_{dc}$ with cryostat temperature (K) shown for each of the 6 laser fluences in the range 0.3 to 5.2 μJ cm^{-2} on thin film sample P1

incorporate that information as a summary. Figure 17 (below) shows the interesting variation of TR-mmWC response ratio as a function of cryostat temperature color coded for laser intensities. In general, the conductance does increase with fluence but, a discontinuity occurs at 55.2K and 151.5K possibly due to alterations in the mobility due to phase transitions.[2, 3]

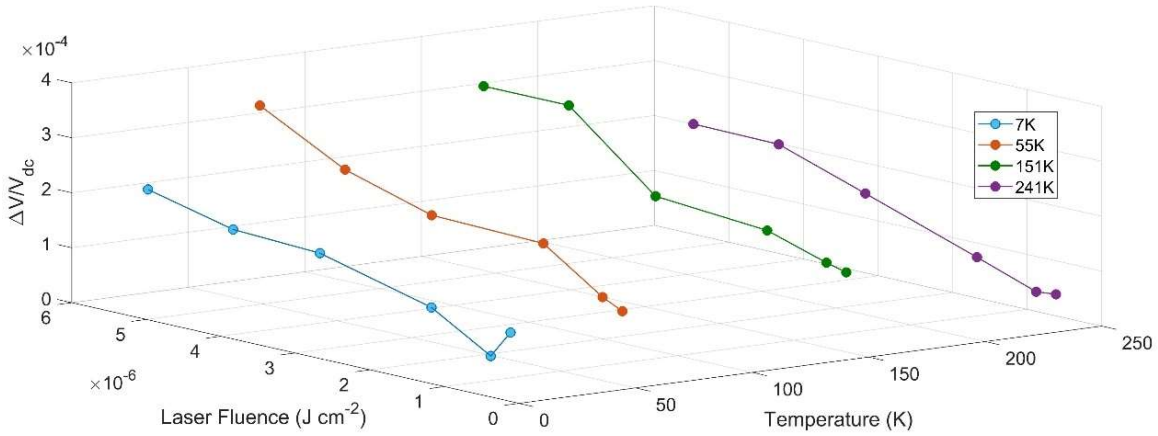

Fig. 18 Variation of P1 sample mmW responses shown as function of laser fluence and cryostat temperature in 3D projection. Note high gains at 51, and 151K at full laser intensities.

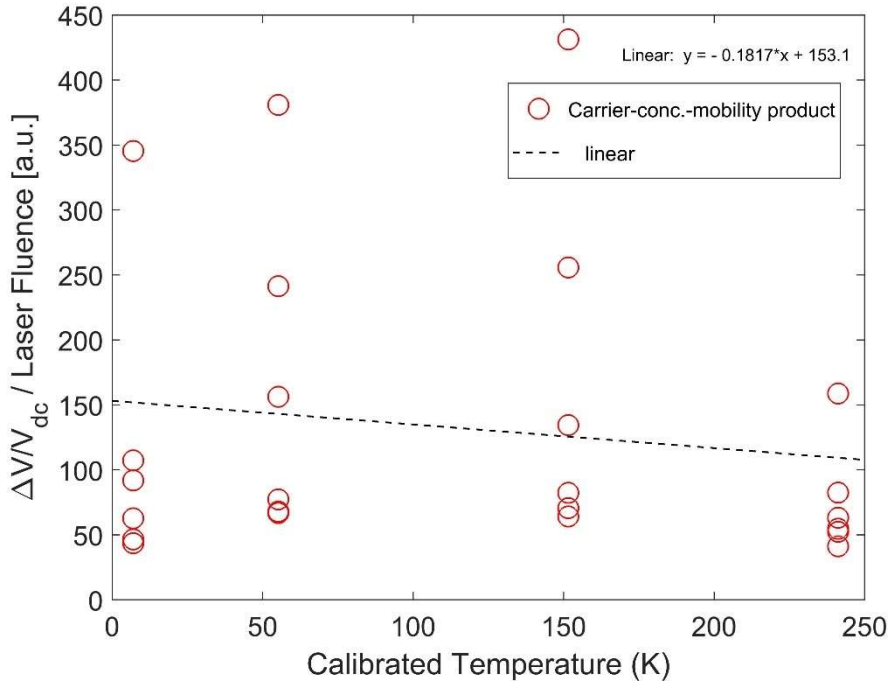

Fig. 19 Variation of P1 sample product of carrier concentration-mobility ($\phi\Sigma\mu$) (qualitative), ratio of TR-mmWC response ratio and the laser fluence, as function of cryostat temperature.

Figure 18 shows the 3D picture of the variation of TR-mmWC response ratio as a function of laser fluence for each of the 4 temperature levels that the sample P1 was subjected to while performing measurements. It is noted that the response is higher at 55.2K and 151.5K. Figure 19 shows the temperature variation of the variable C in the relationship between TR-mmWC response ratio and laser fluence (F), with K (instrument response constant as unity):

$$\Delta V/V_{dc} = -KCF; \quad C = \left[\frac{e(\mu_{e+}\mu_h)Z_0}{h\nu n}\right]\left(\frac{S}{T}\right) \qquad (1)$$

C is the slope of the response-fluence plot. Eqn. (1) involves 'e' as electronic charge, μ_e, and μ_h being the electron and hole mobility, Z_0 being impedance of free space (376.73 Ω), hν being photon energy, and n being the refractive index of the sample at probe frequency, 120GHz. S/T is a ratio of the multiple reflections 'S' (due to the etalon formation of the sample on the substrate) and the transmission (T) parameter (defined in Ref. 1). Variation of slow to fast decay coefficients with temperature is shown in Figs. 20 for each of the laser fluence levels.

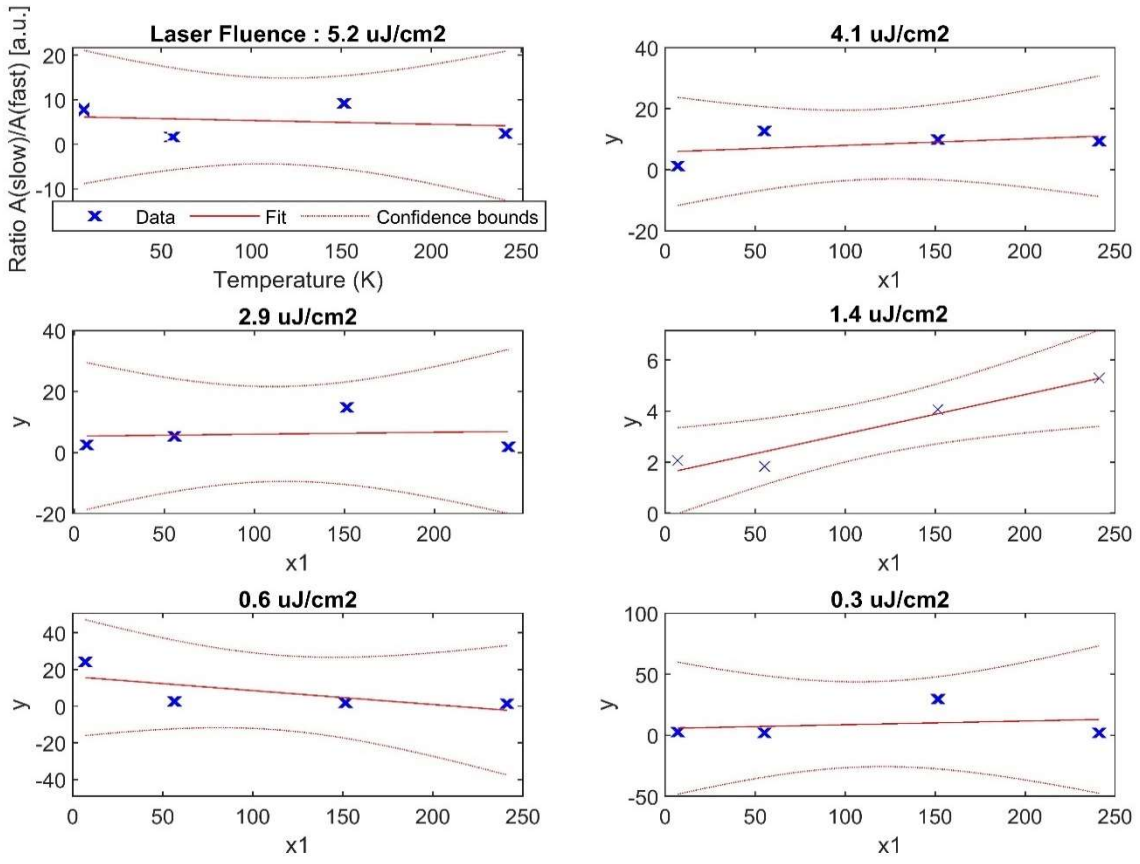

Fig. 20 Variation of ratio of slow to fast coefficients 'a' and 'b' with cryostat temperature for all 6 laser fluence levels separately. The dotted red curves around the linear best fit shows the 95% confidence bound. Note: the increasing trend for 1.4 μJ/cm^{2}fluence might represent changes in the temperature dependent Urbach Energy.

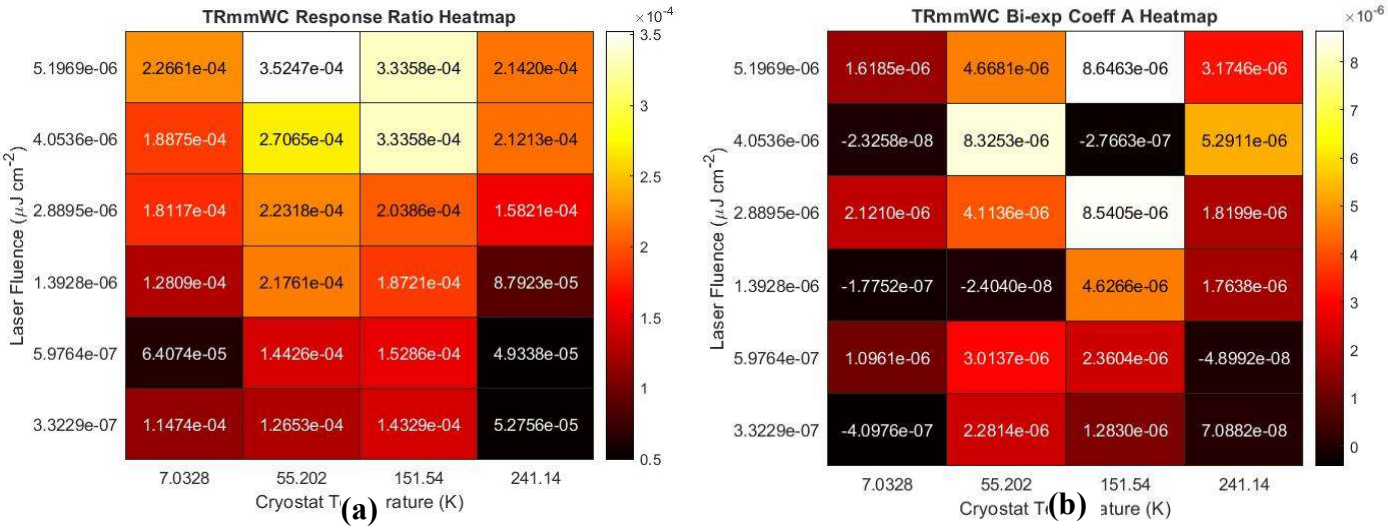

In figures 21 (a)-(e) we show the color heatmaps of each of the bi-exponential fit coefficients as a function of cryostat temperature. We note that the coefficients 'a' and 'b' peak at relatively higher fluences whereas the time constants increase at moderate to lower fluences. The figures below explain each feature discussed earlier and the figure captions explain as much as possible about our inferences.

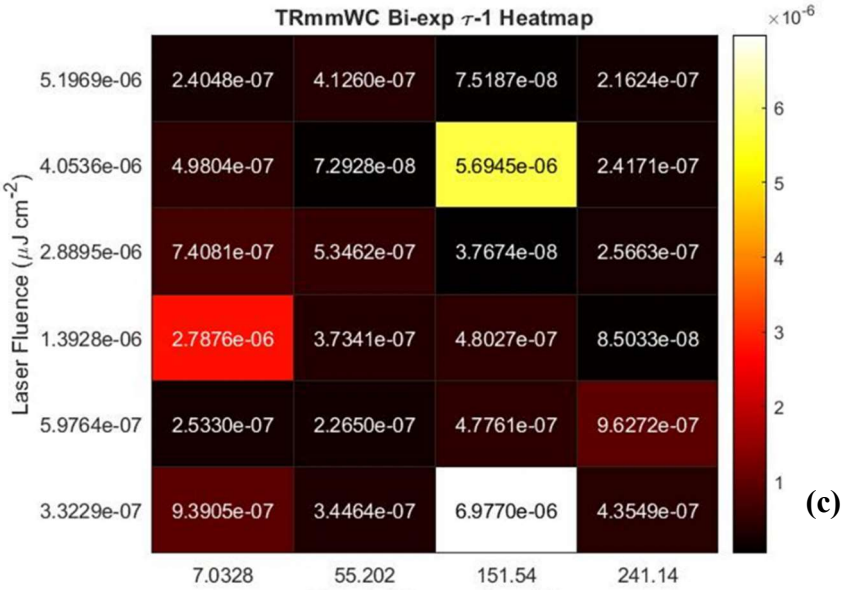

(c)

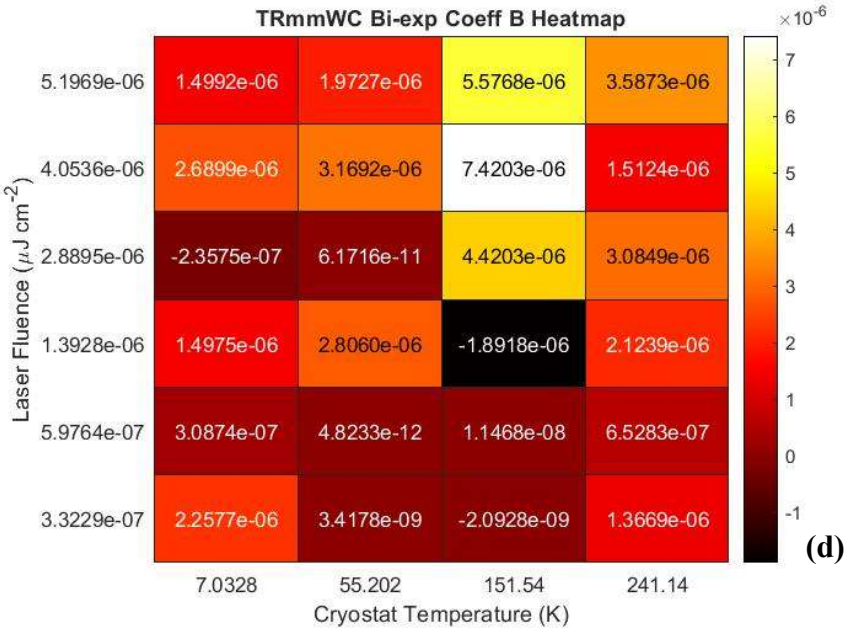

(d)

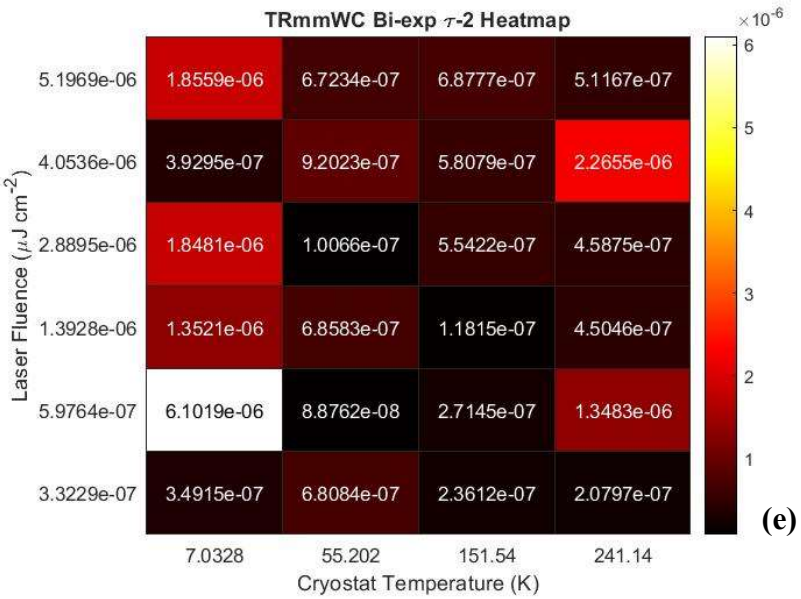

Fig.21 (a) – (e) Heatmaps of bi-exponential coefficients (color) with cryostat temperature-Laser Fluence for sample P1

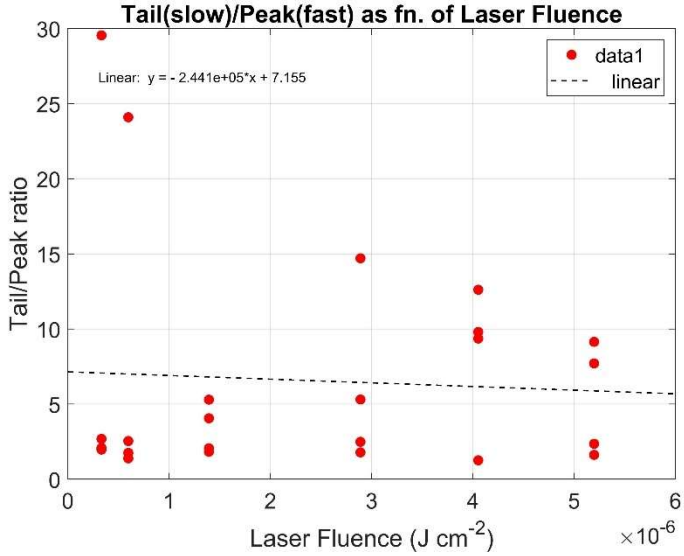

Fig. 22 Tail (slow) to peak (fast) coefficient ratio b/a with laser fluence (all fluences combined) for sample P1.

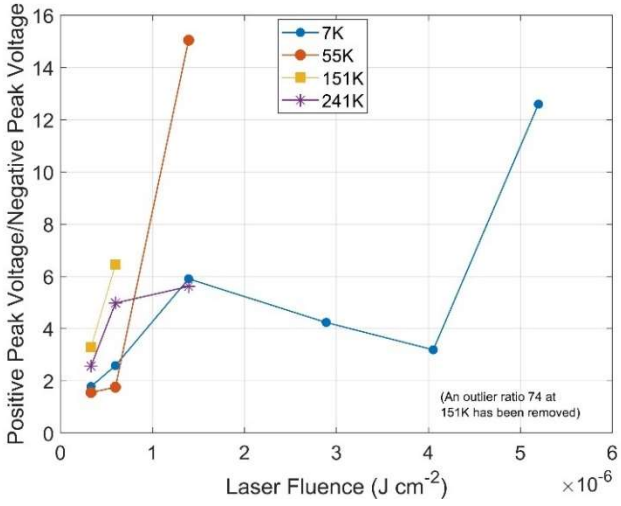

Fig. 23 Ratio of positive, to negative peak voltages in RF transients as function of laser fluences by temperature (color coded) for sample P1. Note: most peaks at moderate temps at lower fluences, Very low temperature yields peak at higher fluence.

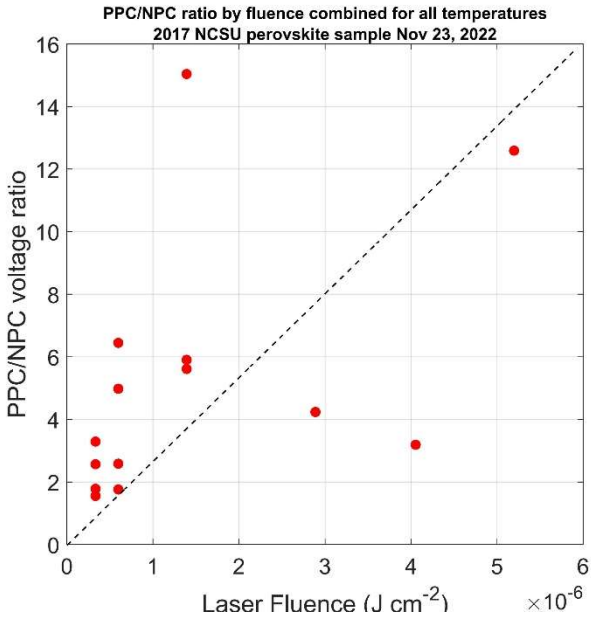

Fig. 24 Positive to negative peak ratio plotted against fluence (fluences combined for all temperatures) for sample P1.

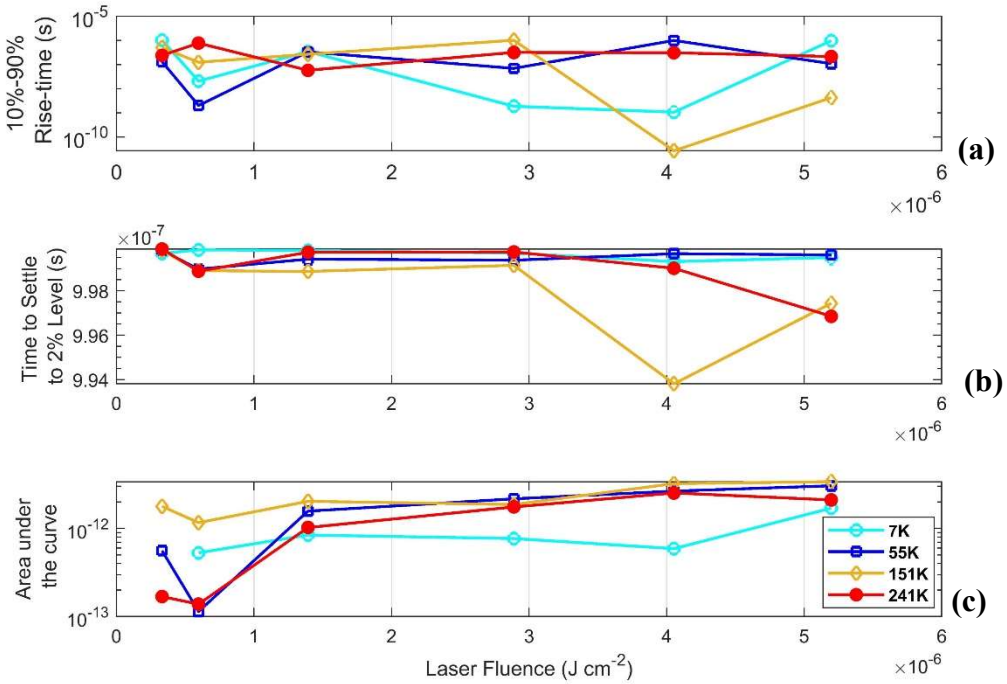

Fig. 25 (a) 10-90% rise-time of sample P1 as function of fluence by temperature (color), We consider rise-time a property of the aging MAL3I since the resistive and capacitive property of the hybrid structure could evolve with time, (b) Time to settle to 2% level, and (c) area under the curve against fluence for sample P1.

An Arrhenius type of plot showing the rate of carrier conc.-mobility product ($\phi\Sigma\mu$) that changes with temperature show a small spike at a higher temperature when the structure of MAL3I is expected to be tetragonal, more so in the cubic-tetragonal transition state possibly. The product, however, shows a decreasing trend while the structure is orthorhombic.

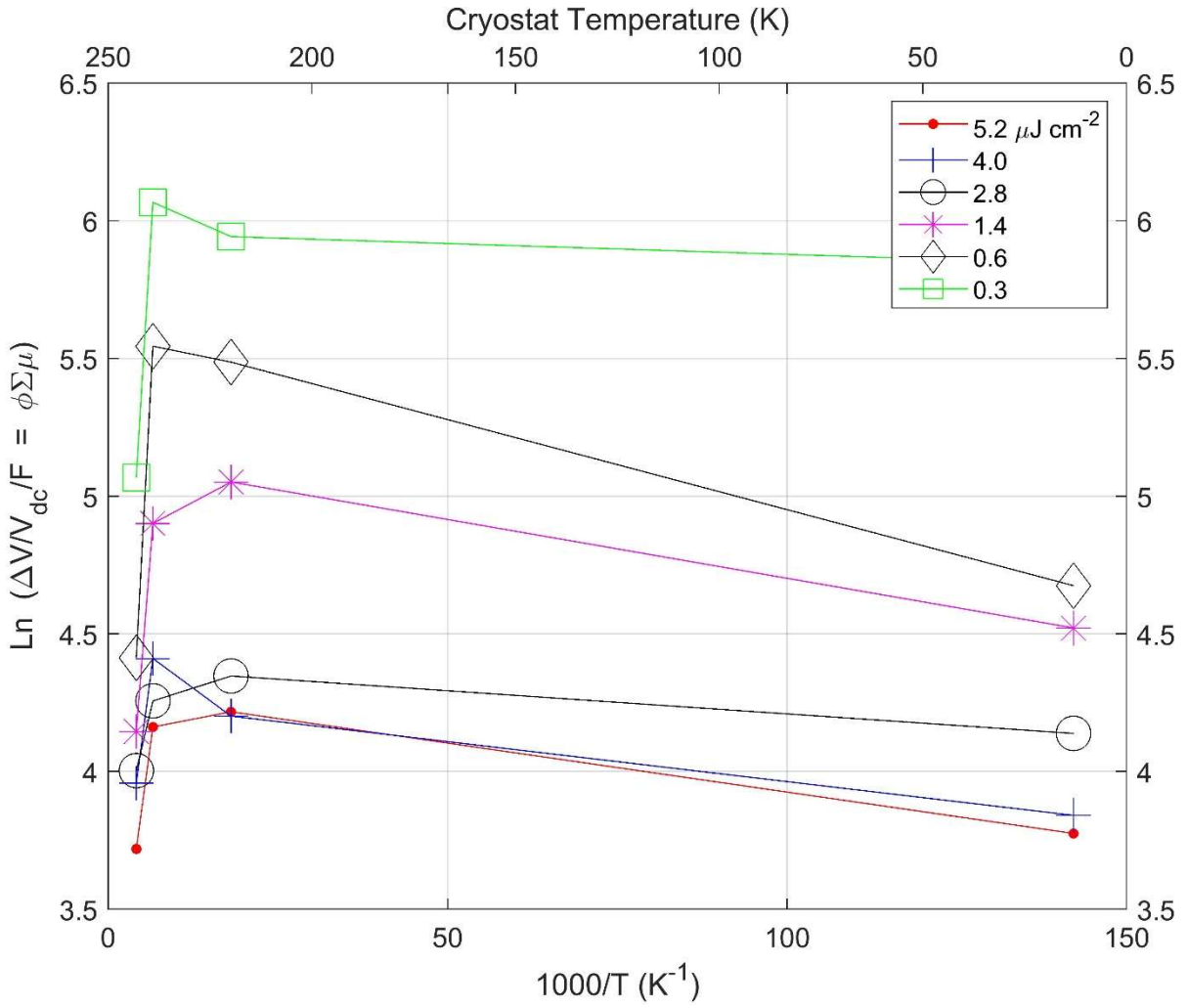

Fig. 26 Shows the variation of the log of the mmW carrier concentration-mobility product with 1000/T (axis 1) for sample P1. Corresponding cryostat temperatures are shown on axis 2 (top); Note the sharp increase of the conductivity of P1 thin film at very low temperatures between 0-50K, and peaks increasing with a decrease in laser fluence F.

1.6 Some preliminary datasets obtained for samples P2, P3, and P4

1.6.(a) $MAPbI_3$ perovskite and $CsPbBrI_2$ thin films made on 08/25/2022

Samples of hybrid P2 (MA perovskite) and completely inorganic perovskite P3 (Cs-$PbBrI_2$) were created by Dr. Franky So's group at NC State University department of materials science (through collaboration with Drs. Rui Su and J. Chiang). For redundancy, two identical samples of P2, and P3 were created by the NCSU group. Sample P4 was created at the Duke University Shared Materials Instrumentation Facility (by Dr. Mark Walters & his group involving Dr. Jay Dalton and Dr. T. Tyler of SMIF). There was the cost involved in obtaining XRD profiles of the sample P4 accomplished at SMIF. However, there was no cost involved in obtaining the P2 and P3 samples at NCSU as we had collaborated intending to publish results together. An excellent set of temperature-dependent mmW response data can be obtained through this STIR program resolving the samples P1, P2, and P3 for their microwave charge dynamical properties when the sample transitions from Orthorhombic-Tetragonal-

Cubic transitions using the in-house calibrated cryostat. Some of the results for P2, P3, and P4 are presented in this section.

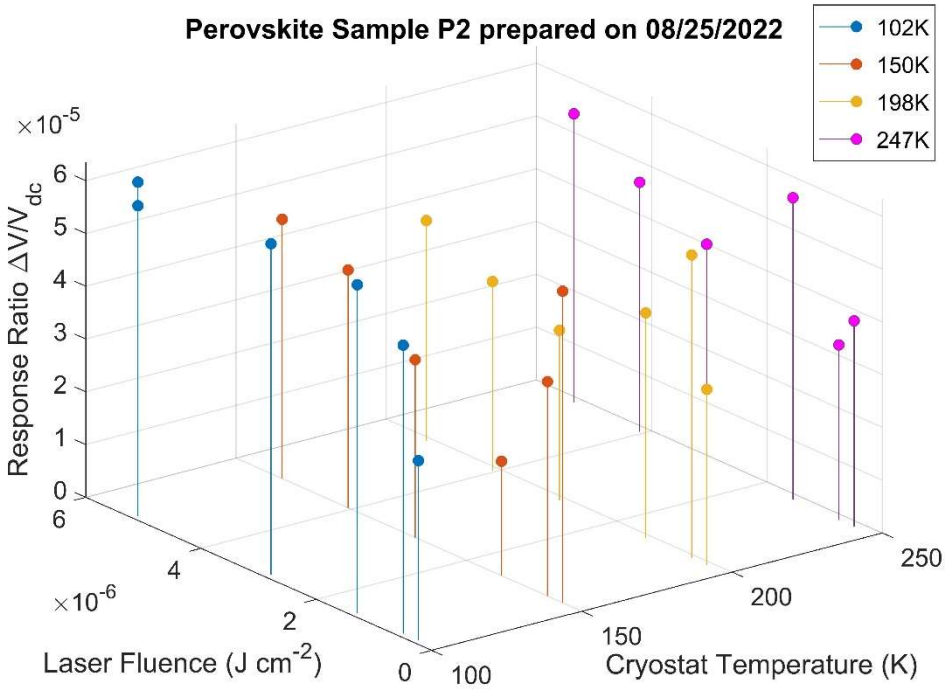

Fig. 27 A 3D stem plot showing the magnitudes of the TR-mmWC response ratio (measure of mmPCD) for the sample P2 (an MAL3I perovskite) as function of laser fluence at each of the the 4 cryostat temperature (color coded). 150K regime shows an increasing trend with lowering of the laser fluence.

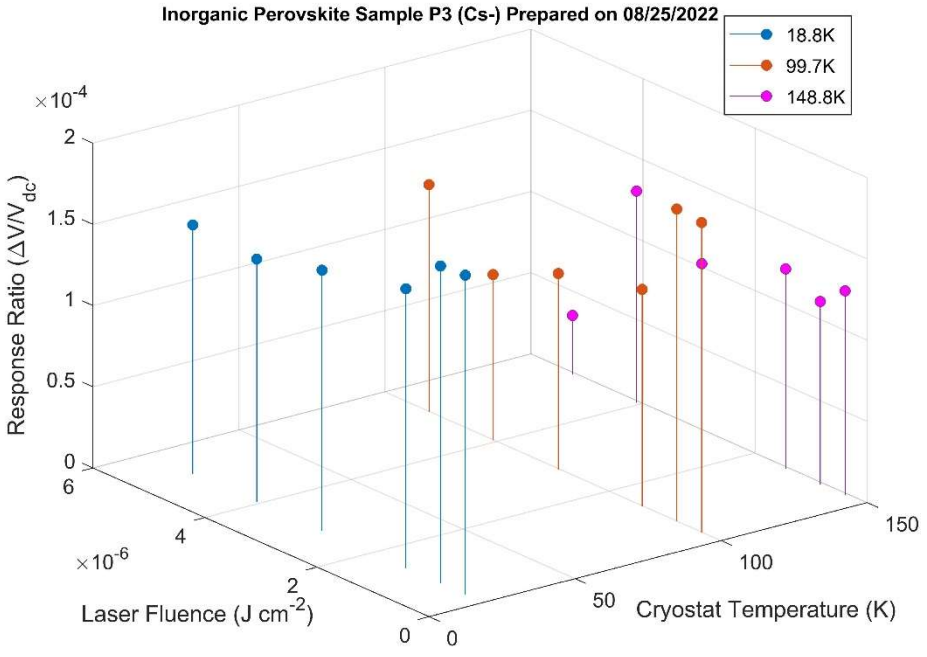

Fig. 28 A 3D stem plot showing the magnitudes of the TR-mmWC response ratio (measure of mmPCD) for the sample P3 (an inorganic $CsPbBrI_2$ perovskite) as function of laser fluence at each of the 3 cryostat temperature (color coded). 100K regime shows an increasing trend with lowering of the laser fluence.

1.6 (b) Very thick (800nm) $MAPbI_3$ perovskite thin film (P4 sample) made on 03/13/2023 using Osilla, Ltd. (UK) precursor solution

An 800nm thick MA perovskite film was spun on a sapphire substrate and Xrad Diffraction results were collected at the Duke Shared Materials Instrumentation Facility (SMiF). The RF transient was obtained by probing at 120GHz and pumping at 266nm, with photon energy far above the MA perovskite band gap. The RF decay curve (Fig. 29) was fitted using bi-exponential fitting and the fit coefficients are shown in figure 29 (below). It needs to be pointed out that background noise was removed using a 7th-order Savitzky-Golay filter with a frame length of 999 designed around these datasets to yield a very good quality noise-free signal. Final signal is obtained after removing the background (no laser) signals (also Savitzky-Golay filtered) through the sample at room temperature only. The film was spun coated at 1000 rpm for 30 seconds and then baked at 100C for 10min. Toluene was not added at the 8th second of the spin process. However, it reveals a very good signal to work with. X-Ray diffraction patterns obtained immediately after the preparation of this P4 sample are also shown in Figure 30.

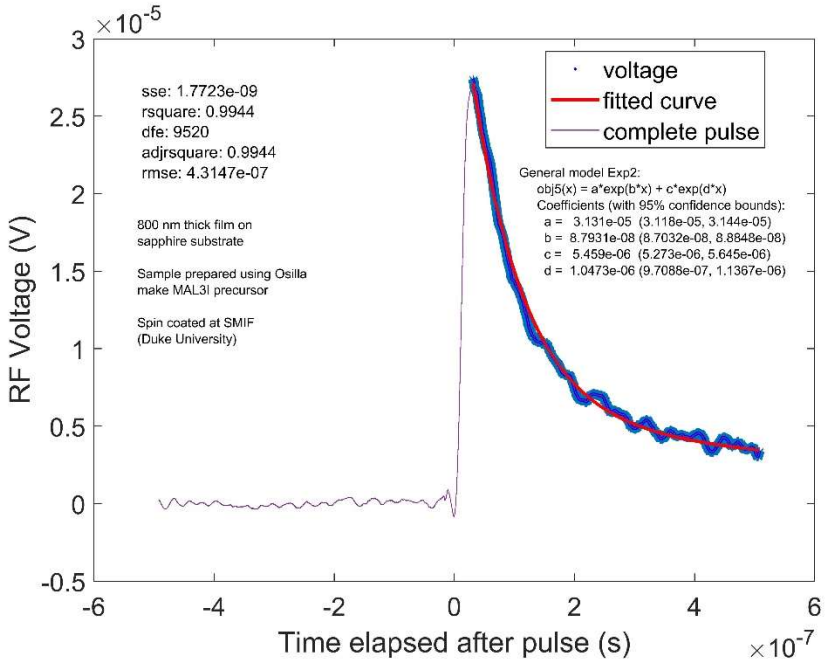

Fig. 29 The 120 GHz RF transient of the sample P4 created on 03/13 (after subtracting the background radiation signals) and bi-exponentially fitted to reveal the coefficients and time constants for mmPCD decay. This data would be useful for analysing the extent of SRH, and trap/defect assisted non-radiative processes and correlate with its hybrid structure.

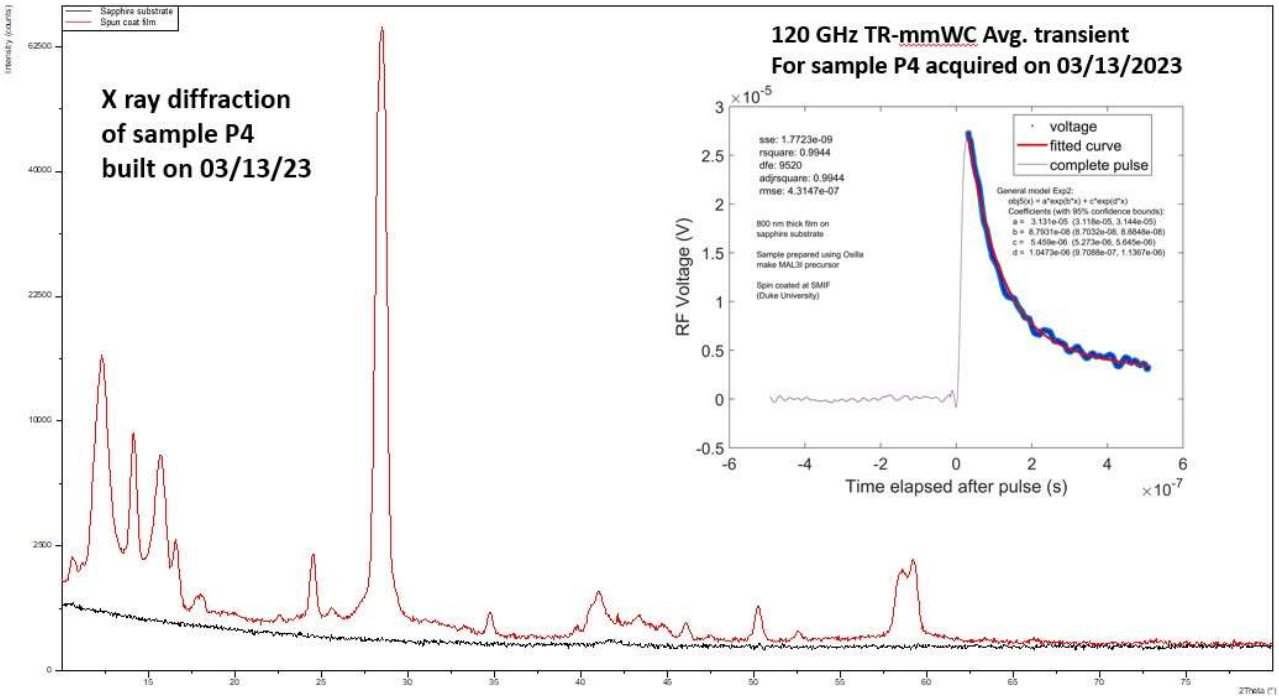

Fig. 30: X-ray diffraction pattern obtained for the sample P4 using the Panalytical X'Pert PRO MRD HR XRD System, Inset: shows the time-resolved millimeter-wave conductance averaged voltage profile when the sample is excited at full laser intensity ~5 uJ cm^{-2} for 266 nm laser beam. XRD obtained at room temperature conforms to its tetragonal structure.

2.0 DC transmission coefficients of samples P1, P2, P3, P4, PCBM and $HfSe_2$

Transmission voltages at 120 GHz were measured once without the sample (free space) and another time, placing the sample in the probe beam path (perpendicular). Reflection losses are accounted for by calculating the transmission coefficients of each sample which are tabulated below.

Table II: DC transmission coefficients of the perovskite, PCBM, and $HfSe_2$ samples prepared.

Sample probed @ 120 GHz	V0=DC voltage at detector no sample (free space)	DC voltage through sample (substrate + thin film) mV	V0 adjusted for surface reflection loss (5% to 8%)	Transmission coefficent for glass slide (Tsubstrate)	Transmission coefficient of thin film (=DC through sample/(V0adjusted* Tsubstrate)	*Samples*
Glass	401.20	289.90	421.26	0.688	NA	*Glass substrate*
P1 on glass	444.00	216.20	466.20	0.688	0.674	*MA perovskite created 2017*
P2 on glass	400.00	172.00	420.00	0.688	0.595	*MA perovskite created 2022*
P2 (extra sample) on glass	401.20	175.70	421.26	0.688	0.606	*MA perovskite created 2022*
P3 on glass	401.20	185.70	421.26	0.688	0.641	*Cs perovskite sample created 2022*
P3 (extra sample)	401.20	191.40	421.26	0.688	0.660	*Cs- perovskite created 2022*
P4 on sapphire	358.10	321.40	376.01	0.980	0.872	*MA perovskite created 2023*
PCBM on glass	401.20	186.60	421.26	0.688	0.644	*PCBM sample created 2022*
PCBM (extra sample) on glass	401.20	187.70	421.26	0.688	0.647	*PCBM sample created 2022*
HfSe2 on Nitto tape	353.00	219.40	370.65	Unknown	0.592	*Hafnium di-selenide film created 2023*

3.0 Attempts with PCBM and $HfSe_2$ materials

3.1 PCBM thin film using powder (Osilla)

250 mg of the solubilized version of Buckminsterfullerene $C_{72}H_{14}O_2$ full name: [6,6]-Phenyl-C61-butyric acid methyl ester was obtained from Osilla, Ltd. This is primarily an electron acceptor material. Due to its tunability of the band structure by electron beam irradiation and its high ON/OFF ratio (~10^4) and suitability as a field effect transistor material, we wanted to study the carrier dynamics of the material using TR-mmWC and before and after irradiation with a 50 keV electron beam.[14,15] For this purpose we dissolved PCBM powder in chlorobenzene and created the precursor solution and created the PCBM thin film on a sapphire substrate using the air control spin coat hood at 1000 RPM (200/s) for the 30s, and then fabricated a metal frame 1.93mm x 2.33mm involving photolithography, evaporation and lift-off process (to create an opaque frame to perform electron beam lithography using the Elonix ELS-7500 EX E-Beam Lithography System at SMIF. Figure 31 shows the photograph of the PCBM film sample produced for this purpose.

Following the production of the bare film and UV-Vis photo spectrometry was performed to reveal the band gap energy in the 200 nm-3µm range. The EBL was run for 8.5 hours total time (8.12h exposure at 20 nA current would supply ~ 13,000 µC/cm^2, with this in mind, we conducted all the processes and used a few chemicals such as Methyl-3 methoxy propanoate (MMP) (for photoresist) TMAH (from developer) and acetone (solvent to remove photoresist) and isopropyl alcohol as a solvent to clean after acetone.

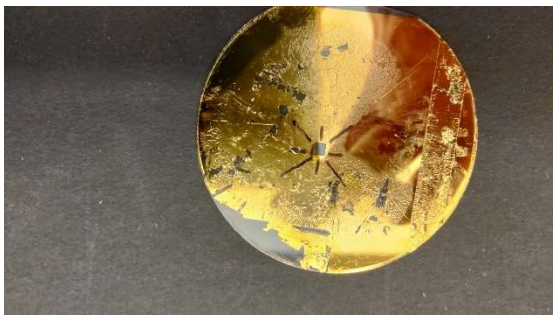

Fig. 31 Spin coated PCBM film on sapphire with a gold foil protecting layer. The EBLwindow based on the metal frame/lift off produced is also seen. This sample was subjected to UV-Vis before 8.5 hours of EBL and after EBL. No data could be recorded band gap before and after EBL for this PCBM film. The PCBM on EBL window is supposedly etched off due to acetone application in photoresist removal process.

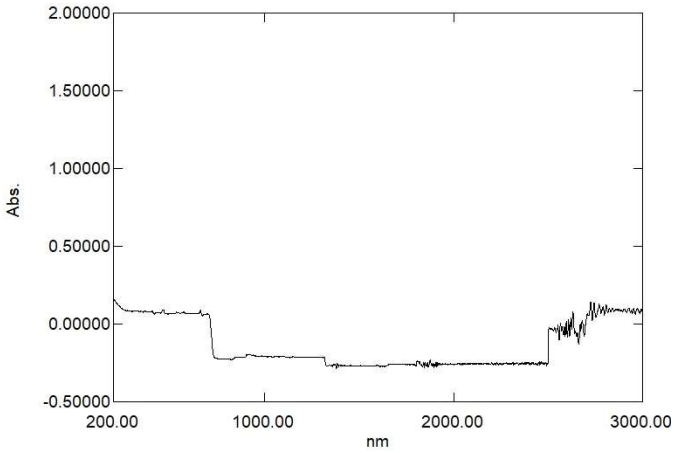

Fig. 32 UV-Vis absorption profile of the PCBM film before EBL

Figure 32 shows the UV-Vis results on the spin-coated PCBM film before overnight exposure in the electron beam system, and after overnight exposure in the electron beam system. There is little to no absorption and no significant difference in the data (other than noise where gratings switched). It looks like the data pertains to just the bare sapphire substrate. From this data and a visual inspection of the sample, we believe that the hard mask processing that was done after the PCBM was applied likely dissolved the PCBM film from the open area. The mask was made using a liftoff process and utilized acetone to remove the resist over the open area. We believe that the acetone also removed the PCBM

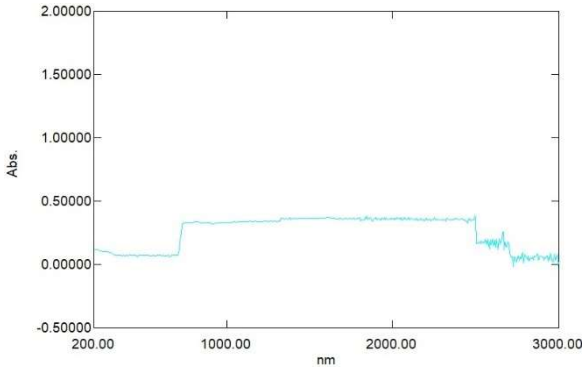

Fig. 33 UV-Vis absorption profile after EBL. There is no absorption for PCBM seen

film. The film was brought back to the lab for TR-mmWC and the transmission at 120GHz show the characteristic of sapphire substrate only. So, we need to repeat this experiment without doing the hard mask processing that involved acetone. Our idea is to machine a hard mask with a small (~2mm) opening and affix it to the spun-coated film. This will avoid all solvents once the film is coated, and we believe we can make the EBL exposure work with the hard mask affixed.

3.2 $HfSe_2$ film using crystals (Osilla)

Indirect band (1.1 eV) Group IV Transition metal dichalcogenide (TMD) 2D semiconductor Hafnium di-selenide[16,17] was selected to study its charge carrier dynamics in the D band mmW and when exposed to various operable temperature range 200K-300K and acquire a well-suited dataset for its application as Field Effect Transistor (FET) material using prefabricated test chips. For this purpose, we acquired $HfSe_2$ small crystals from Osilla, Ltd., and using Nitto tapes, we attempted to transfer the material on to glass substrate for performing TRmmWC analysis. However, it was found that the small crystals were very difficult to transfer to the glass slides using the scotch tape method. Solution processing of this sample was not attempted since we currently do not have solution processing capability. None of the Molecular Beam Epitaxy film growers agreed to prepare this sample for us. Hence, we tried to use the blobs of small crystals that were adhered to the Nott tape while attempting the scotch tape method of transfer, to perform the TR-mmWC analysis. For this we have used 266nm pumps and 532 nm pumps but, unfortunately, we did not find any TR-mmWC response at 120 GHz. We, however, could only collect the DC transmission data and came up with a transmission coefficient of 0.592 at 120 GHz. The film on Nitto tape is shown in Figure 34.

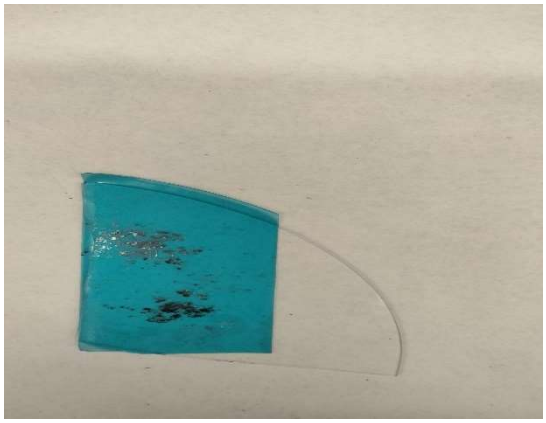

Fig. 34 Small crystals of $HfSe_2$ attached to the nitto tape (blue) which was used to acquire the DC transmission coefficient data.

A proposal has been approved by the Penn State University 2D crystal consortium (2DCC) for the production of films of $HfSe_2$ for our work at NCCU but, it would take some time to get the data since the sample is currently being prepared at 2DCC. We hope to narrow this down to get a 2D thin film of $HfSe_2$ prepared either in-house or at the 2DCC laboratory for our proposed work.

A collaborative effort was made to observe the degrading tendency (growth of bubbles in $HfSe_2$ films over time) hence, we used a silicon substrate and a thin film was collected just by contact method with the small crystals. The film was subjected to atomic force microscopy (AFM) attached to the SNOM system available at NCCU (PI: Dr. Marvin Wu and post-doctoral scholar: Dr. Clayton Casper). This attempt revealed an interesting profile as shown in Fig. 35 (below).

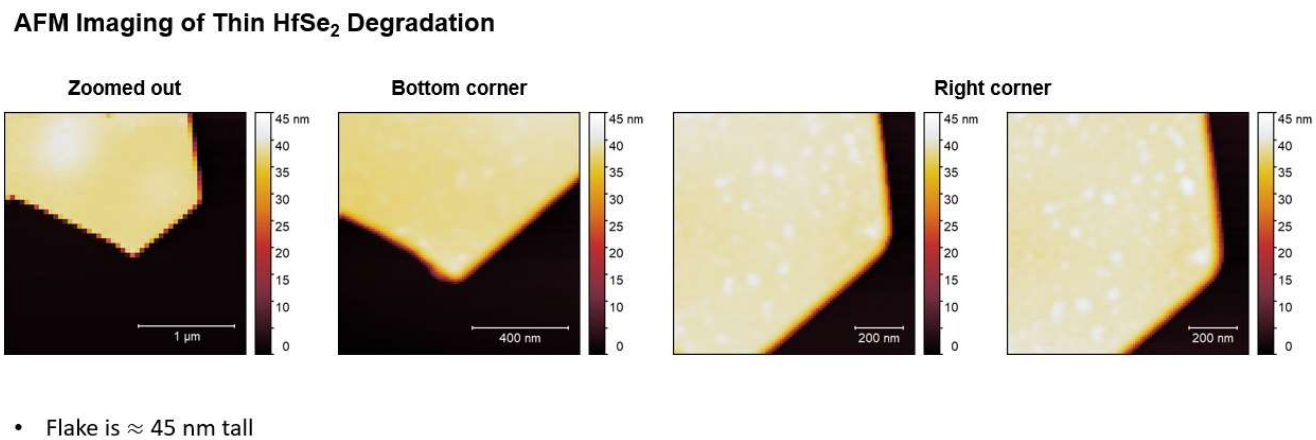

Fig. 35 AFM images of $HfSe_2$ on silicon in chronological order

4.0 Future

Field Effect Transistor (FET) analysis using the 3D form of the materials can be performed only after all the structural and millimeter-wave charge dynamical characteristics are acquired successfully. Here, we have progressed well in the direction of completing this project, but time limitations and resource management have been in the way of completing all the goals of this project in the specified time. In the future, we can carry on this work at least for the perovskite samples (through current small grant catalyst funding from NSF) produced using the proven techniques learned in the experimental phases to achieve results in this STIR project. However, a substantial set of TRmmWC response data collected for perovskites under sweeping temperature and laser fluence is a very important resource that was acquired through this STIR grant.

Most importantly, we have built confidence in using the cryostat-based mmW differential absorption data acquisition system mainly because we find the current technique to be very responsive to changes in laser fluence and temperature as well. We believe that, in the future, with this setup, it would be possible to acquire very high-quality structural-mmW property data by its functionality (such as field-effect) of novel semiconductors. We also plan to incorporate a suitable interferometer with the apparatus for the measurement of the dielectric property of the material at every probe frequency, and, also, will attempt to measure, and acquire structural changes radiative decay signals while the experiment is implemented.

References

1. Roy, B., Jones, C.R., Vlahovic, B., Ade, H.W., and Wu, M.H., A time-resolved millimeter wave conductivity (TR-mmWC) apparatus for charge dynamical properties of semiconductors, *Rev. Sci. Instrum*., **2018** Vol. *89*, 104704.
2. Bojtor, A., Kollarics, S., Markus, B.G., Sienkiewicz, A., Kollar, M., Forro, L., and Simon, F., Ultralong charge carrier recombination time in methylammonium lead halide perovskites, *ACS Photonics*, **2022** *9*, 3341.

3. Millot, R.L., Eperon, G.E., Snaith, H.J., Johnston, M.B., and Herz, L.M., Temperature-dependent charge-carrier dynamics in $CH_3 NH_3 PbI_3$ perovskite thin films, *Adv. Func. Mat.,* **2015**, *25*, 6218-6227.
4. Findik, G., Biliroglu, M., Seyitliyev, D., Mendes, J., Barrette, A., Ardekani, H., Lei, L., Dong, Qq., So, F., and Gundogdu, K., High-temperature superfluorescence in methyl ammonium lead iodide, *Nature Photonics*, **2021**, *15*, 676-680.
5. Johnston, M.B., and Herz, L., Hybrid perovskites for photovoltaics: charge-carrier recombination, diffusion, and radiative efficiencies, *Acc. Chem., Res*. **2016**, *49*, 146-154.
6. Pisoni, A., Jacimovic, J., Barisic, O.S., Spina, M., Gaal, R., Forro, L., and Horvath, E., Ultra-low thermal conductivity in organic-inorganic hybrid perovskite $CH_3 NH_3 PbI_3$, *J. Phys. Chem. Lett.,* **2014**, *5*, 2488-2492.
7. Ng C.H., Ripolles, T.S., Hamada, K., Teo, S.H., Lim, H.N., Bisquert, J., and Hayase, S., Tunable open circuit voltage by engineering inorganic cesium lead bromide/iodide perovskite solar cells, *Scientific Reports*, **2018,** *8* 2482.
8. Zhao, D., Sexton, M., Park, H-Y, Baure, G., Nino, J.C., and So, F., High-efficiency solution-processed planar perovskite solar cells with a polymer hole transport layer, *Adv. Energy Mater*., **2015**, *5*, 1401855.
9. M. Biliroglu, Findik, G., Mendes, J., Seyitliyev, D., Lei, L., Dong, Q., Mehta, Y., Temnov, V., So, F., and Gundoglu, K., Room-temperature superfluorescence in hybrid perovskites and its origins, *Nature Photonics,* **2022**, *16*, 324-329.
10. Roy, B. Vlahovic, B., and Wu, M.H. "Supervised learning applied to high-dimensional millimeter wave transient absorption data for age prediction of perovskite thin-film" arXiv:2211.02431 [cond-mat.mtrl-sci], **2022,** DOI: https://doi.org/10.48550/arXiv.2211.02431.
11. Zhang, N., Xiong, J., Zhong, J., and Leatham, K., Gaussian Process Regression Method for Classification for High-Dimensional Data with Limited Samples, *2018 Eighth International Conference on Information Science and Technology (ICIST)*, Cordoba, Granada, and Seville, Spain, **2018**, pp. 358-363, doi: 10.1109/ICIST.2018.8426077.
12. Roy, B. Jingshan, C. Rui, S., So, F. and Wu, M.H., Comparison of time-resolved millimeter-wave responses between aged and new perovskite thin films. TechRxiv. Preprint. **2023,** https://doi.org/10.36227/techrxiv.22082360.v1 (*Journal: undecided*)
13. Roy, B. and Wu, M.H. On using pump-fluence swept TRmmWC temperature transients data to directly infer charge carrier mobility, (in preparation for Journal to be communicated: *Appl. Phys. Rev.)* **2023.**
14. Yoo, S.H., Kum, M.J., and Cho, S.O, Tuning electronic band structures of PCBM by electron irradiation, *Nanoscale Research Letters*, **2011**, *6*, 545.
15. Hauff, E.v., Dyakonov, V., and Parisi, J., Study of field effect mobility in PCBM films and P3HT: PCBM blends, *Solar Energy Materials & Solar Cells,* **2005**, *87* 149-156.
16. Aretoulli, K.E., Tsipas, P., Tsoutsou, D., Marquez-Velasco, J., Xenogiannapoulou, E., Giamini, S.A., Vassalou, E., Kelaidis, N., and Dimoulas, A., Two-dimensional semiconductor $HfSe_2$ and $MoSe_2$/$HfSe_2$ van der Waals heterostructures by molecular beam epitaxy, *Appl. Phys. Lett.,* **2015**, *106*, 143105.
17. $HfSe_2$ thin films: 2D transition metal dichalcogenides grown by molecular beam epitaxy, *ACS Nano*, **2015**, *9, 1,* 474-480.

What opportunities for training and professional development has the project provided?

One graduate student of NCCU has been trained to use the TRmmWC apparatus and the cryostat operation for data acquisition at fixed probe frequency. He has also been exposed to data analysis methods and computation of the time domain data-derived charge dynamical parameters of interest.

How were the results disseminated to communities of interest?

In-house and local university collaborators were sent the data either as attachments to emails or sometimes when the volume is larger, by sharing files using dropbox.

What do you plan to do during the next reporting period to accomplish the goals and

Nothing to report.

OPTIONAL CATEGORIES

PRODUCTS: What has the project produced?

A set of very high-quality temperature-dependent time-resolved millimeter wave charge-carrier dynamical data at 120 GHz for perovskite will form a strong basis for foundational studies related to mmW structure-property relationships for FET functionality.

Journal publications.

Three journal articles are prepared. Two have already been published on preprint servers, one in ArXiV (Cornell University preprint server) and another on TechRXiv (IEEE), One being prepared. Full acknowledgments are/will be made to each of these publications, except in Chitara et al. (2023):

Roy, B., Vlahovic, B., and Wu, M.H. "Supervised learning applied to high-dimensional millimeter wave transient absorption data for age prediction of perovskite thin-film" arXiv:2211.02431 [cond-mat.mtrl-sci], https://doi.org/10.48550/arXiv.2211.02431. (*Journal: undecided*), **2022**.

Roy, Biswadev; Chai, Jingshan; Su, Rui; So, Franky; Wu, Marvin, Comparison of time-resolved millimeter-wave responses between aged and new perovskite thin films. TechRxiv. Preprint. https://doi.org/10.36227/techrxiv.22082360.v1 (*Journal: undecided*), **2023**.

Roy, B., and Wu, M.H., On using pump-fluence swept TRmmWC temperature transients data to directly infer charge carrier mobility, (in preparation for Journal to be communicated: *Appl. Phys. Rev.),* **2023**

Chitara, B., Roy, B., Yan, F., and Wu., M.H., Facile synthesis and morphology-induced photoconductivity modulation of Bi_2O2S nanostructures, *Materials Lett.,* **2023**, (being revised).

Books or other non-periodical, one-time publications.

B. Roy, B. Vlahovic, M.H. Wu and C.R. Jones, "Charge dynamical properties of photo-responsive and novel semiconductors using time-resolved millimeter-wave apparatus", **book chapter for** *Spectroscopy and Characterization of Nanomaterials and Novel Materials. Experiment, Modeling, Simulations, and Applications* (Ed. P. Misra) Wiley *published* (2021)

Acknowledgement of federal support from this project: No

Other publications, conference papers and presentations.

None

Website(s) or other Internet site(s)

None

Technologies or techniques

Developed a unique free-space TRmmWC temperature data acquisition using a cryostat

Inventions, patent applications, and/or licenses

None

Other products

Identify any other significant products that were developed under this project. Describe the

product and how it was shared. Examples of other products are:

x□ data or databases;

Completely new datasets were archived on pump fluence-swept temperature-based mmW response data and DC characterization using the free space geometry and use of a cryostat in line with the existing TRmmWC apparatus.

x□ software;

Developed a Matlab-based algorithm and code to automatically compute the bi- or tri-exponential fitting of TRmmWC datasets along with automatic data filtering and acquisition of signal step-response and related parameters along with spectrogram, periodogram, and frequency effects, including machine learning regression analysis of aging semiconductors.

x□ instruments or equipment;

Temperature data recording and calibration of cryostat was a new addition to the TRmmWC apparatus methods.

PARTICIPANTS & OTHER COLLABORATING ORGANIZATIONS: Who has been involved?

 What individuals have worked on this project?

Mainly PI himself, Dr. Marvin H. Wu and Dr. Clayton Casper of NCCU, Dr. F. So and Dr. Rui Su of NCSU (mainly for the preparation of samples P1, P2, and P3), and Duke University SMIF personnel Dr. Mark Walters, Dr. Jay Dalton and Dr. T. Tyler (for production of sample P3, and attempt to perform EBL on PCBM film).

 Has there been a change in the active other support of the PD/PI(s) or senior/key

personnel since the last reporting period?

No

 What other organizations have been involved as partners?

NCSU, Duke University, SMIF

 Have other collaborators or contacts been involved?

No

What individuals have worked on this project?

Project Roles:

PD/PI : Dr. Biswadev Roy

Co PD/PI: None

Faculty: Dr. Marvin H. Wu; helped in the development of cryostat and its working components, and low-temperature manual calibration process, and attempted to use the $HfSe_2$ sample to get AFM corroboratory data.

Community College Faculty: None

Technical School Faculty: None

K-12 Teacher: None

Postdoctoral (scholar, fellow or other postdoctoral position): None

Other Professional: None

Technician: None

Staff Scientist (doctoral level): None

Statistician: None

Graduate Student (research assistant): None

Non-Student Research Assistant: None

Undergraduate Student: None

Technical School Student: None

High School Student: None

Consultant: None

Research Experience for Undergraduates (REU) Participant: None

Other (specify): None

Has there been a change in the active other support of the PD/PI(s) or senior/key personnel since the last reporting period?

"Nothing to Report."

What other organizations have been involved as partners?

"Nothing to Report."

Have other collaborators or contacts been involved?

"Nothing to Report."

IMPACT: What was the impact of the project? How has it contributed?

This project enabled high-quality temperature data acquisition (first time using millimeter wave free space probing method) for perovskites, PCBM, and $HfSe_2$ all high switching speed materials of interest in the development of field-effect applications.

What was the impact on the development of the principal discipline(s) of the project?

"Nothing to Report."

What was the impact on other disciplines?

"Nothing to Report."

What was the impact on the development of human resources?

"Nothing to Report."

What was the impact on teaching and educational experiences?

"Nothing to Report."

What was the impact on physical, institutional, and information resources that form infrastructure?

"Nothing to Report"

What was the impact on technology transfer?

"Nothing to Report"

What was the impact on society beyond science and technology?

"Nothing to Report"

What percentage of the award's budget was spent in foreign country(ies)?

None

CHANGES/PROBLEMS

"Nothing to Report,"

Changes in approach and reasons for change

Not Applicable

Actual or anticipated problems or delays and actions or plans to resolve them

Not Applicable

Changes that had a significant impact on expenditures

Not Applicable

Significant changes in use or care of human subjects, vertebrate animals, biohazards, and/or select agents

None

SPECIAL REPORTING REQUIREMENTS

None